Available online at www.sciencedirect.com
SCIENCE DIRECT
ELSEVIER
Behavioural Brain Research 172 (2006) 272–277
BEHAVIOURAL BRAIN RESEARCH
www.elsevier.com/locate/bbr

Research report

Decreased prefrontal activation during letter fluency task in adults with pervasive developmental disorders: A near-infrared spectroscopy study

Hitoshi Kuwabara [a,b,*], Kiyoto Kasai [a], Ryu Takizawa [a], Yuki Kawakubo [a], Hidenori Yamasue [a], Mark A. Rogers [a], Michiko Ishijima [a], Keiichiro Watanabe [a], Nobumasa Kato [a]

[a] *Department of Neuropsychiatry, Graduate School of Medicine, University of Tokyo, 7-3-1 Hongo, Bunkyo-ku, Tokyo 113-8655, Japan*
[b] *Department of Psychiatry, Tokyo Metropolitan Umegaoka Hospital, Japan*

Received 8 January 2006; received in revised form 6 May 2006; accepted 10 May 2006
Available online 23 June 2006

Abstract

Functional neuroimaging studies have suggested that dysfunction of prefrontal cortex (PFC) is present in persons with pervasive developmental disorders (PDD). Recently, the development of near-infrared spectroscopy (NIRS) has enabled noninvasive bedside measurement of regional cerebral blood volume. Although NIRS enables the noninvasive clarification of brain functions in many psychiatric disorders, it has not yet been used to examine subjects with PDD. The aim of our study was to conduct an NIRS cognitive activation study to verify PFC dysfunction in PDD. The subjects were 10 adults with PDD and 10 age- and gender-matched healthy subjects. Hemoglobin concentration changes were measured with a 24-channel NIRS machine during the letter fluency task. While the number of words generated during the letter fluency task did not differ significantly between groups, the analysis of covariance including IQ as a confounding covariate showed that the PDD group was associated with bilateral reduction in oxy-hemoglobin concentration change as compared with the control group. The statistical results did not change when only IQ-matched high-functioning subjects ($N=7$) were included. Moreover, reduced oxy-hemoglobin concentration change for the right PFC was significantly correlated with verbal communication deficits within the PDD group. The present findings are consistent with proposed prefrontal dysfunction in PDD subjects identified by other neuroimaging modalities. The present results may be also potentially useful for applying NIRS to clinical settings of child psychiatry.

Keywords: Pervasive developmental disorders (PDD); Near-infrared spectroscopy (NIRS); Letter fluency task; Prefrontal cortex

1. Introduction

Pervasive developmental disorder (PDD) is defined on the basis of a selected set of behavioral disturbances that more or less map onto specific functional systems of the brain [26]. The difficulties with social reciprocity, communication, and restricted behaviors and interests that occur with PDD suggest that the syndrome affects a functionally diverse and widely distributed set of neural systems [30].

Functional neuroimaging studies have repeatedly suggested that the function of the prefrontal cortex (PFC), critical for working memory and executive functioning [7], is disturbed in persons with PDD. A functional magnetic resonance imaging (fMRI) study using the embedded figure task showed reduced activation of PFC and greater activation of ventral occipitotemporal regions in adults with PDD [25]. An fMRI study showed that autistic adults had significantly less task-related activation in dorsolateral PFC in comparison with healthy adults during a spatial working memory task [16]. An fMRI study reported a variable and scattered representation along the lateral convexity of the frontal and parietal lobes during a visually cued motor sequencing task in adults with autism [22]. Another line of studies have used "theory of mind" tasks to investigate medial PFC abnormalities in PDDs; a pilot positron emission tomography (PET) study of adults with Asperger's disorder showed specific engagement of the medial PFC, except that the center of activation was displaced below and anterior in the patients compared with controls [8], while another PET study showed reduced dorsomedial PFC activation in adults with PDD [4]. In accordance with the latter investigation, a PET study reported

* Corresponding author. Tel.: +81 3 5800 9263; fax: +81 3 5800 6894.
E-mail address: kuwabara@roy.hi-ho.ne.jp (H. Kuwabara).

0166-4328/$ – see front matter © 2006 Elsevier B.V. All rights reserved.
doi:10.1016/j.bbr.2006.05.020

reduced dopaminergic activity in the dorsomedial PFC of autistic children [5].

While functional brain imaging methodologies such as PET and fMRI have excellent spatial resolution, they are limited in that they require large apparatus which prevents their use in a bedside setting for diagnostic and treatment purposes. Recently, the development of near-infrared spectroscopy (NIRS) has enabled noninvasive and bedside measurement of regional cerebral blood volume (rCBV) in terms of the relative concentrations of oxyhemoglobin [oxyHb] and deoxyhemoglobin [deoxyHb].

NIRS is a neuroimaging modality that is especially suitable for psychiatric patients, due to the following reasons [18]. Because NIRS is relatively insensitive to motion artifact, it can be applied to emotional activation that might cause some motion of the subjects. The subject can be examined in a natural sitting position, without any surrounding noise or feeling of obstruction. In addition the cost is much lower than other neuroimaging modalities and the set-up is very easy.

Although NIRS enables the noninvasive clarification of brain functions in many psychiatric disorders, including schizophrenia, bipolar disorder, depression, dementia of Alzheimer type and post-traumatic stress disorder [6,12,17–20,28], NIRS has not yet been applied to examine subjects with PDD. To evaluate [Hb] change in the prefrontal cortex using NIRS, the verbal fluency test has been often used for cognitive activation, since previous NIRS studies have used letter fluency test for cognitive activations, and showed displayable prefrontal activation during the verbal fluency task in healthy subjects [10,11,13]. Thus, the letter fluency test may be considered a valid cognitive activation task to detect PFC dysfunction by NIRS. Therefore we conducted an NIRS cognitive activation study, using letter fluency test, to verify PFC dysfunction in PDD. Based on previous studies using other neuroimaging techniques that showed lateral prefrontal dysfunction during executive tasks in PDD, we predicted that the subjects with PDD would show lower prefrontal [oxy-Hb] change than healthy subjects. We also predicted that decreased [oxy-Hb] would be associated with severity of symptoms in the PDD group.

2. Materials and methods

2.1. Subjects

The subjects were 10 adults with PDD (six men and four women; 18–37 years old) and age- ($t[18]=0.543$, $p=0.594$) and gender- (χ-square test: $p=0.121$) matched healthy subjects (9 men and 1 woman; 24–34 years old). All individuals with PDD were outpatients of the Department of Neuropsychiatry, Tokyo University Hospital, Japan. Healthy subjects were recruited from college students, hospital staff and their acquaintances. PDD subjects were diagnosed according to DSM-IV criteria [1] by two trained child psychiatrists (H.K. and M.I.). Eight patients were taking psychotropic drugs at the time of examination (Table 1). Their psychopathology was assessed with the childhood autism rating scale (CARS)—Tokyo version [15,27]. We used a CARS score of 27 as the cut-off point for autistic disorder [21], but not for Asperger's disorder nor PDD not otherwise specified. All participants were right-handed as based on the Edinburgh Inventory [24]. IQ scores were obtained using the Wechsler Adult Intelligence Scale-Revised. Although the mean IQ was significantly higher in healthy controls than in PDD, 7 out of 10 PDD subjects were high-functioning with IQ > 85 (Table 1). None of the subjects had a history of substance or alcohol abuse or dependence. This study was approved by the Ethical Committee of Faculty of Medicine, University of Tokyo (No. 630), and written informed consent was obtained from all the subjects prior to their participation in the study.

2.2. Activation task

Hemoglobin concentration changes were measured during the letter fluency task, according to a method similar to that of Suto et al. [28]. The subjects sat on a chair with their eyes open throughout the measurements. The cognitive activation consisted of a 30-s pretask baseline, a 60-s letter fluency task, and a 60-s post-task baseline. In the pre- and post-task baseline periods, the subjects were instructed to simply repeat aloud the syllables /a/, /i/, /u/, /e/, and /o/. In the activation-task period, the subjects were instructed to generate as many words whose initial syllable was /a/, /ka/, or /sa/ as they could. The three initial syllables changed in turn every 20 s during the 60-s task, to reduce the time during which the subjects were silent. The subjects were instructed with an auditory cue at the start and end of the task or baseline period and at the change of the designated

Table 1
Clinical and demographic details of the subjects

Case no.	Age	Sex	IQ	Subtype	CARS	Medication (mg/day)	LFT
Pervasive developmental disorder							
PDD1	19	M	132	Au	35	Risperidone 1	14
PDD2	27	M	122	As	26	Levomepromazine 10	19
PDD3	36	F	75	Au	37	Haloperidol 3, valproate 600, paroxetine 10	12
PDD4	21	F	101	As	25.5	Lithium 400	9
PDD5	21	M	59	PDDNOS	28	Pimozide 9, zotepine 300, carbamazepine 600	16
PDD6	25	F	62	Au	29.5	paroxetine 10	15
PDD7	37	M	96	Au	34.5	No medication	12
PDD8	34	F	122	Au	29.5	Pimozide 1	14
PDD9	18	M	101	As	33.5	Lithium 200, paroxetine 20	10
PDD10	27	M	94	Au	31.5	No medication	14
Mean	26.5	M6/F4	96.4		31		13.5
S.D.	7.1		25.1		3.9		2.9
Control subjects ($n=10$)							
Mean	27.9	M9/F1	118.3				15.4
S.D.	4.1		15.2				2.5

CARS, childhood autism rating scale; LFT, letter fluency task; M, male; F, female; Au, autistic disorder; As, asperger disorder; PDDNOS, pervasive developmental disorder not otherwise specified.

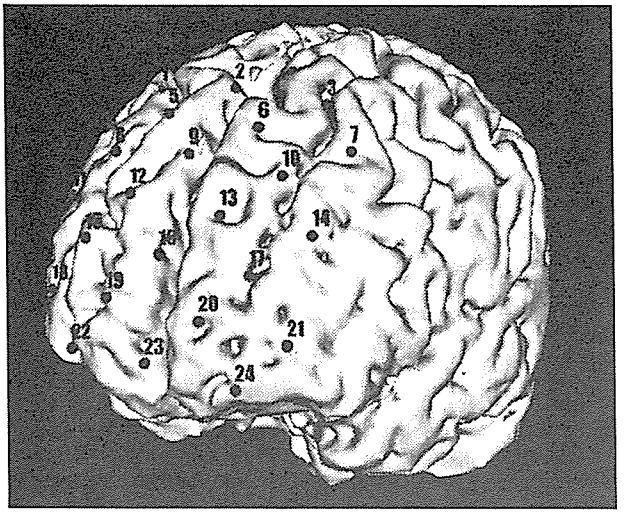

Fig. 1. NIRS measurement points superimposed on a representative subject's 3D-MRI.

syllables. The number of words generated during the letter fluency task was determined as a measure of task performance.

2.3. NIRS measurement

[oxyHb], [deoxyHb], and [totalHb] were measured with a 24-channel NIRS machine (Hitachi ETG-100; Hitachi Medical Corporation, Tokyo, Japan) at two wavelength of near-infrared light (760 and 840 nm). Concentration changes of [oxyHb] and [deoxyHb] were calculated from the difference in the light absorption characteristics of these two hemoglobin species based on Beer–Lambert law. [TotalHb] was calculated as the sum of [oxyHb] and [deoxyHb].

Sixteen probes (eight emitters and eight detectors) were placed over a subject's frontal regions, with the lowest probes positioned along the Fp1–Fp2 line according to the international 10/20 system used in electroencephalography (Fig. 1). The inter-probe distance was 3.0 cm, and the 16 probes can measure [Hb] changes at 24 measurement points in a 9 cm × 9 cm area. The machine measures [Hb] change approximately 2–3 cm beneath the scalp, i.e., the cortical surface area [12].

The absorption of near-infrared light was measured with a time resolution of 0.1 s. Baseline correction was made by using linear fitting based on the two baseline data (the pre-task baseline: the mean across a 10-s period just before the activation period; the post-task baseline: the mean across a 5-s period beginning 50 s after the activation period). This was intended to correct the data during the fluency task for activation due to simple speaking. Moving average methods were used to exclude short-term motion artifacts in the analyzed data (moving average window: 5 s).

2.4. Statistical analysis

[OxyHb] and [deoxyHb] data in each channel were averaged across the two segments (pretask baseline segment and task segment). [OxyHb] or [deoxyHb] at pretask baseline and that at the task period were compared using paired t-test for all channels to test whether [Hb] showed significant changes at the task period relative to the baseline (degree of freedom varied across channels due to a low signal to noise (S/N) ratio at upper prefrontal channels). Low signal to noise ratio was observed at upper frontal channels (channels #1–14) for some subjects, which would substantially reduced the sample size in the repeated measures ANOVA using all 24 channels. Therefore, we adopted repeated measures ANOVA using lower frontal channels (eight channels; left: channels 17, 20, 21, 24; right: 15, 18, 19, 22; approximately Brodmann's areas 10 and 46; see Fig. 1) which had good data for all subjects. More specifically, three-way mixed model repeated measures analysis of covariance (ANCOVA) was performed for [oxyHb] or [deoxyHb] data during the activation-task period, using diagnosis as the between-subject factor, hemisphere and channel as within-subject factors, and IQ as the covariate. To further rule out the effect of IQ, this analysis was repeated for data only including high-functioning PDD subjects ($N=7$; mean IQ = 110 [S.D. = 15], matched with control subjects [$t=1.15$, $p=0.27$]). When the sphericity assumption was violated, Greenhouse–Geisser correction was performed and associated epsilon was reported. We also conducted group comparison of [oxyHb] or [deoxyHb] change using t-tests at each channel.

We performed correlational analysis between task performance and [oxyHb] change at channels #15, 17, 18, 19, 20, 21, 22, and 24 for the control group, PDD group, or for the combined subjects using Pearson's correlation.

In the PDD group, exploratory correlational analyses were performed between the averaged [oxyHb] data during task segment across left 4 (channels 17, 20, 21, 24) or right 4 (channels 15, 18, 19, 22) channels and scores on each item of the CARS using Spearman's rho.

3. Results

The number of words generated during the letter fluency task showed no statistically significant differences between the groups (PDD group: mean 13.5, S.D.: 2.9; control group: mean 15.4, S.D.: 2.5; comparison: $t[18]=1.56$, $p=0.14$).

In the control group, [oxyHb] rapidly increased immediately after the start of the task period, was maintained at the activated level during the task period, and decreased gradually after the task was finished. In the control group, [oxyHb] change showed a significant increase during the activation period relative to the pretask period for 18 of 24 channels, while the [deoxyHb] did not show significant decrease for any channel. These results confirmed that the task employed in this study produced measurable increase in [oxyHb] in healthy subjects. In the PDD group, [oxyHb] showed a very slight increase, and decreased immediately after the end of the task period (Fig. 2). All PDD subjects showed similar waveforms (Fig. 3).

For [oxyHb], the ANCOVA revealed a significant main effect of "diagnosis" ($F[1,17]=6.45$, $p=0.021$). There was no significant diagnosis-by-hemisphere ($F[1,17]=0.005$, $p=0.95$), diagnosis-by-channel ($F[3,51]=0.926$, $p=0.41$; $\varepsilon=0.713$), or diagnosis-by-hemisphere-by-channel ($F[3,51]=0.676$, $p=0.50$; $\varepsilon=0.598$) interaction. There was no significant main effect of hemisphere ($F[1,17]=0.058$ $p=0.81$) or channel ($F[3,51]=0.150$, $p=0.87$; $\varepsilon=0.713$). For subset of data only including high-functioning subjects, the statistical conclusion did not change (diagnosis main effect: $p=0.035$; diagnosis-by-hemisphere interaction: $p=0.99$; diagnosis-by-channel interaction: $p=0.45$; diagnosis-by-hemisphere-by-channel interaction: $p=0.57$; hemisphere main effect: $p=0.15$; channel main effect: $p=0.32$). The t-test at each channel showed that the PDD group had decreased [oxyHb] than the control group at channels no. 4, 10, 11, 14–22, and 24, most of which were lower frontal channels that were included in the repeated measures ANCOVA. The PDD group did not show increased [oxyHb] than the control group at any channel.

For [deoxyHb], the repeated measures ANCOVA did not show a significant main effect or interactions. The t-test at each channel showed that there was no significant difference between groups for any channel except for channel no. 4 (control: mean [deoxyHb], 0.0616; PDD: mean, −0.0452; $p=0.045$). However, this significance was driven by a significant increase of

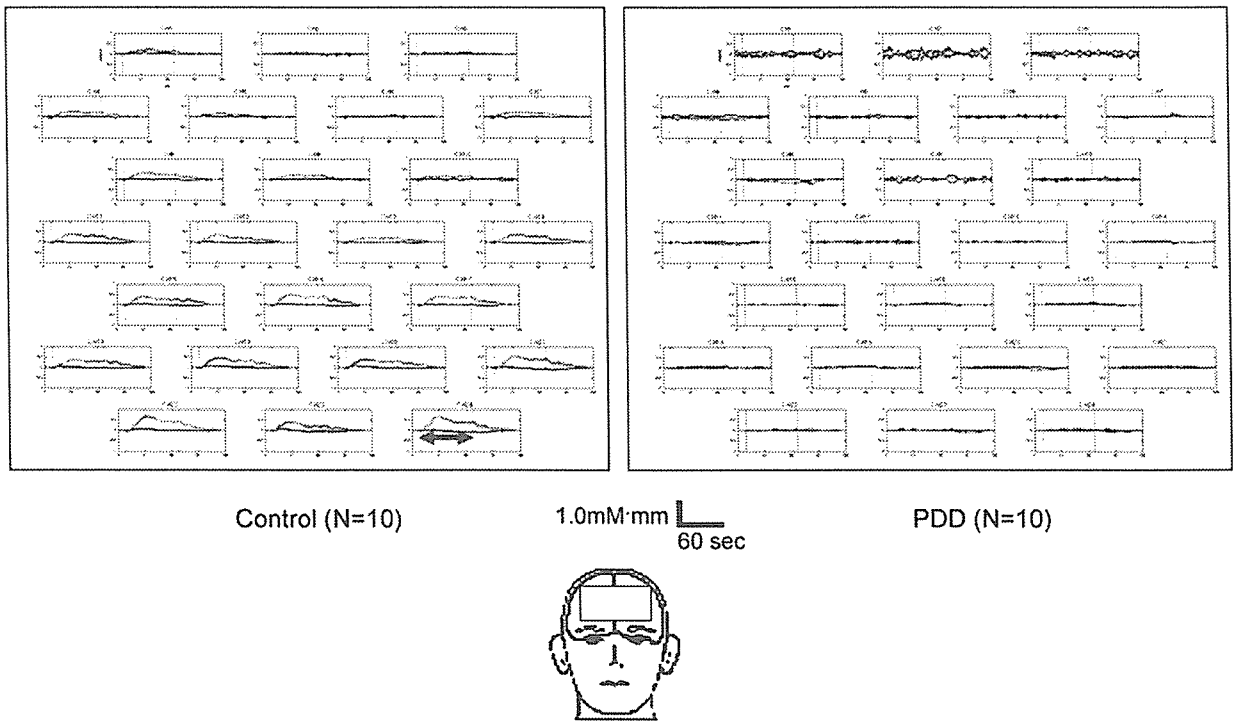

Fig. 2. Grand average waveforms of hemoglobin concentration changes during cognitive activation for controls ($N=10$) and PDDs ($N=10$). [OxyHb], red line; [deoxyHb], blue; and [totalHb], green. The red arrow indicates the period of cognitive activation.

[deoxyHb] at this channel in the control group (paired t-test, $p=0.050$), which is difficult to interpret and is likely to be driven by a type I error.

For association between task performance and [oxyHb] change, there was no significant correlation for any channel for the PDD or control subjects. However, there were significant correlation for channels #15, 17, 19, 20, 21, and 24 for the combined subjects (p's = 0.012–0.049) although these correlations did not remain significant after Bonferroni correction. It is likely that these trends in the combined subjects but not in the separate group were spuriously driven by the consistently lower [oxyHb] change in the PDD group.

Correlational analysis between [oxyHb] and CARS showed that [oxyHb] for the right hemisphere was negatively correlated with "verbal communication" score on the CARS (rho = −0.652, $p=0.041$) in the PDD group, although this correlation did not remain significant after Bonferroni correction for multiple comparisons.

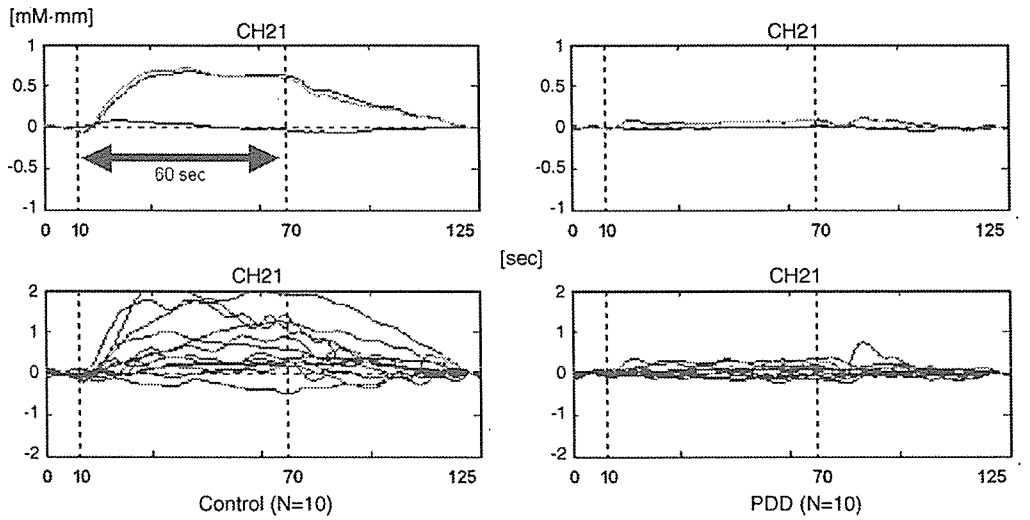

Fig. 3. Upper: grand average waveforms for [oxyHb] (red line), [deoxyHb] (blue), and [totalHb] (green) shown for a representative channel (channel 21; left DLPFC). Lower: [oxyHb] for each subject superimposed. The red arrow indicates the period of cognitive activation.

4. Discussion

To our knowledge, this is the first NIRS study that evaluated prefrontal activation in individuals with PDD. The present findings are consistent with the proposed prefrontal dysfunction in PDD subjects identified by other imaging modalities, such as fMRI and PET. Depressed prefrontal blood volume change in PDD during an executive task is congruent with fMRI studies which reported decreased activation in PFC during executive function tasks [16,25]. However, this result is incongruent with an fMRI study by Müller et al. [22] which reported increased activation in PFC during a visuomotor task, and with an fMRI study by Baron-Cohen et al. [2] who reported decreased activation in the amygdale but not the PFC of adult PDDs during social cognitive tasks. This difference may be partly explained by the difference in the tasks employed, and this difference indicates that the PFC dysfunction of adult PDDs may be task specific.

For clinical implications, our preliminary analysis showed that lower [oxyHb] in the right prefrontal cortex during letter fluency task predicted worse verbal communication scores in individuals with PDDs. However, these results should be considered to be tentative, since the analysis was exploratory in nature.

Possible explanations should be discussed for our observation of significantly depressed prefrontal blood volume change during the letter fluency task in spite of preserved task performance. There may be two possible interpretations. First, the PDD subjects may use alternative cognitive strategies that activate different brain regions, such as lateral and medial temporal lobe, to compensate for the task performance. Consistent with this interpretation, it has been noted that successful performance on the word fluency task, which includes a letter fluency task, may depend on the ability to produce clusters of related responses, and reduced clustering had been reported in PDD [3,29]. Ring et al. [25] showed reduced activation in PFC and increased activation in occipitotemporal regions during the embedded figure task in PDD. They proposed that differences in functional anatomy might indicate that the cognitive strategies adopted by PDD group were different from those adopted by the normal group. Happé et al. [8] employed a "Theory of Mind Task" and found that both a PDD group and a control group showed task-related activation in regions immediately adjacent to the left medial prefrontal cortex, but that only the control group showed significant activity in the left medial prefrontal cortex itself. Their explanation was that PDD subjects were using a more general purpose reasoning mechanism in order to infer mental states. However, because of limited coverage of measurement areas, the present study cannot fully rule out the possibility that other areas such as superior temporal cortex may play a compensatory role thus resulting in the preserved task performance we observed.

Another explanation for significant difference in [oxyHb] change despite preserved task performance may be possible. The underactivation of the prefrontal cortex, compromising verbal communication ability as assessed by CARS in the PDD subjects, may not be sufficient to impair more elementary executive task performance such as an easier version of letter fluency task used in the present study. These possibilities should be further tested in studies manipulating task difficulty and using NIRS with a denser and wider probe array.

NIRS enables measurement of Hb concentration changes not as absolute values but as those relative to pretask baseline. Therefore we cannot empirically rule out the possibility that the present findings may be due to a difference in prefrontal blood volume in the pretask period (i.e., *hyper*perfusion in the pretask period in PDD). However, single photon emission computed tomography studies have found significant *hypo*perfusion during the resting state in the frontal areas of PDD children [9,14,23,31,32] and adults [32] as compared to normal controls. Thus, decreased activation during the cognitive task was not likely to be due to saturated hemodynamic state in the pretask baseline in PDD.

Other methodological considerations of our study need to be commented upon. First, our sample of PDD included some low-functioning subjects. However, we carefully controlled the effect of IQ by using ANCOVA model as the statistical analysis, and by conducting confirmatory analysis with high-functioning subjects only. Thus, IQ may not be a major confounding factor in the present study. Second, the inclusion of medicated subjects may confound the results. However, although the small sample size of the divided PDD subgroups according to medication status (medicated, $N=8$; unmedicated, $N=2$) did not permit strict statistical analysis, the medicated and unmedicated subgroups did not significantly differ in [oxyHb] change for left nor right PFC (averaged values as used in the correlational analysis; Mann–Whitney U-test, p's = 0.60 and 0.60, respectively). Third, because of small sample sizes, the present study could not refer to the difference between Autistic disorder, Asperger's disorder and PDD not otherwise specified. Further research will be necessary to clarify this point. Finally, Hermann et al. [11] found left hemispheric predominance for [oxyHb] change during VFT in healthy subjects. However, Suto et al. [28] and Kameyama et al. [13], which used the similar task procedure to ours and Japanese subjects showed bilateral activation. The discrepancy may be explained by difference in task procedure and language.

In conclusion, to our knowledge this is the first study which evaluated prefrontal activation using NIRS in individuals with PDD. Although the mechanism behind depressed blood volume change during letter fluency task remains unclear, the present results point to be potential for gainful application of NIRS in clinical settings of child psychiatry.

Acknowledgements

This study was supported by Grants from the Ministry of Health, Labour and Welfare, Japan (to KK and NK), and in part by Grant-in-Aid for Scientific Research for Young Investigators (to YK) from the MEXT, Japan. MR was supported by a Postdoctoral fellowship from the Japan Society for the Promotion of Science (P 05234).

References

[1] Amercian Psychiatric Association. Diagnostic and statistical manual of mental disorders. 4th ed. Washington, DC: American Psychiatric Association; 1994.

[2] Baron-Cohen S, Ring HA, Wheelwright S, Bullmore ET, Brammer MJ, Simmons A, et al. Social intelligence in the normal and autistic brain: an fMRI study. Eur J Neurosci 1999;11:1891–8.
[3] Boucher J. Word fluency in high-functioning autistic children. J Autism Dev Disorder 1988;18:637–45.
[4] Castelli F, Frith C, Happé F, Frith U. Autism, Asperger syndrome and brain mechanisms for the attribution of mental states to animated shapes. Brain 2002;125:1839–49.
[5] Ernst M, Zametkin AJ, Matochik JA, Pascualvaca D, Cohen RM. Low medial prefrontal dopaminergic activity in autistic children. Lancet 1997;350:638.
[6] Fallgatter AJ, Roesler M, Sitzmann L, Heidrich A, Mueller TJ, Strik WK. Loss of functional hemispheric asymmetry in Alzheimer's dementia assessed with near-infrared spectroscopy. Cognit Brain Res 1997;6:67–72.
[7] Goldman-Rakic PS. Regional and cellular fractionation of working memory. Proc Natl Acad Sci USA 1996;93:13473–80.
[8] Happé F, Ehlers S, Fletcher P, Frith U, Johansson M, Gillberg C, et al. Theory of mind in the brain. Evidence from a PET scan study of Asperger syndrome. NeuroReport 1996;8:197–201.
[9] Hashimoto T, Sasaki M, Fukumizu M, Hanaoka S, Sugai K, Matsuda H. Single-photon emission computed tomography of the brain in autism: effect of the developmental level. Pediatr Neurol 2000;23:416–20.
[10] Herrmann MJ, Ehlis AC, Fallgatter AJ. Frontal activation during a verbal-fluency task as measured by near-infrared spectroscopy. Brain Res Bull 2003;61:51–6.
[11] Herrmann MJ, Walter A, Ehlis AC, Fallgatter AJ. Cerebral oxygenation changes in the prefrontal cortex: effects of age and gender. Neurobiol Aging, 2005 [Epub ahead of print].
[12] Hock C, Villringer K, Muller-Spahn F, Wenzel R, Heekern H, Schuh-Hofer S, et al. Decrease in parietal cerebral hemoglobin oxygenation during performance of a verbal fluency task in patients with Alzheimer's disease monitored by means of near-infrared spectroscopy (NIRS)—correlation with simultaneous rCBF-PET measurements. Brain Res 1997;755:293–303.
[13] Kameyama M, Fukuda M, Uehara T, Mikuni M. Sex and age dependencies of cerebral blood volume changes during cognitive activation: a multichannel near-infrared spectroscopy study. Neuroimage 2004;22:1715–21.
[14] Kaya M, Karasalihoğlu S, Üstün F, Gültekin A, Çermik TF, Fazlioğlu Y, et al. The relationship between 99mTc-HMPAO brain SPECT and the scores of real life rating scale in autistic children. Brain Dev 2002;24:77–81.
[15] Kurita H, Miyake Y, Katsuno K. Reliability and validity of the childhood autism rating scale—Tokyo version (CARS-TV). J Autism Dev Diord 1989;19:389–96.
[16] Luna B, Minshew NL, Garver KE, Lazar NA, Thulborn KR, Eddy WF, et al. Neocortical system abnormalities in autism. An f MRI study of spatial working memory. Neurology 2002;59:834–40.
[17] Matsuo K, Kato N, Kato T. Decreased cerebral haemodynamic response to cognitive and physiological tasks in mood disorders as shown by near-infrared spectroscopy. Psychol Med 2002;32:1029–37.
[18] Matsuo K, Kato T, Taneiichi K, Matumoto A, Ohtani T, Hamamoto T, et al. Activation of the prefrontal cortex to trauma-related stimuli measured by near-infrared spectroscopy in posttraumatic stress disorder due to terrorism. Psychophysiology 2003;40:492–500.
[19] Matsuo K, Taneichi K, Matumoto A, Ohtani T, Yamasue H, Sakano Y, et al. Hypoactivation of the prefrontal cortex during verbal fluency test in PTSD: near-infrared spectroscopy study. Psychiatr Res: Neuroimag 2003;124:1–10.
[20] Matsuo K, Watanabe A, Onodera Y, Kato N, Kato T. Prefrontal hemodynamic response to verbal-fluency task and hyperventilation in bipolar disorder measured by multi-channel near-infrared spectroscopy. J Affect Disord 2004;82:85–92.
[21] Mesibov GB, Schopler E, Schaffer B, Michal N. Use of childhood autism rating scale with autistic adolescents and adults. J Am Acad Child Adolesc Psychiatr 1989;28:538–41.
[22] Müller RA, Kleinhans N, Kemmotu N, Pierce K, Courchene E. Abnormal variability and distribution of functional maps in autism: an fMRI study of visuomotor learning. Am J Psychiatr 2003;160:1847–62.
[23] Ohnishi T, Matsuda H, Hashimoto T, Kunihiro T, Nishikawa M, Uema T, et al. Abnormal regional cerebral blood flow in childhood autism. Brain 2000;123:1838–44.
[24] Oldfield RC. The assessment and analysis of handedness: the Edinburgh inventory. Neuropsychologia 1971;9:97–113.
[25] Ring HA, Baron-Cohen S, Wheelwright S, Williams SCR, Brammer M, Andrew C, et al. Cerebral correlates of preserved cognitive skills in autism. A functional MRI study of embedded figure task performance. Brain 1999;122:1305–15.
[26] Rutter M. The Emanuel Miller memorial lecture 1998 Autism: two-way interplay between research and clinical work. J Child Psychol Psychiatr 1999;40:169–88.
[27] Schopler E, Reichler RJ, DeVellis RF, Daly K. Toward objective classification of childhood autism: childhood autism rating scale (CARS). J Autism Dev Disord 1980;10:91–103.
[28] Suto T, Fukuda M, Ito M, Uehara T, Mikuni M. Multichannel near-infrared spectroscopy in depression and schizophrenia: cognitive brain activation study. Biol Psychiatr 2004;55:501–11.
[29] Turner M. Generating novel ideas: fluency performance in high-functioning and learning disabled individuals with autism. J Child Psychol Psychiatr 1999;40:189–201.
[30] Volkmar FR, Autism. Lancet 2003;362:1133–41.
[31] Wilcox J, Tsuang MT, Ledger E, Algeo J, Schnurr T. Brain perfusion in autism varies with age. Neuropsychobiology 2002;46:13–6.
[32] Zibovicius M, Garreau B, Samson Y, Remy P, Barthelemy C, Syrota A, et al. Delayed maturation of the frontal cortex in childhood autism. Am J Psychiatr 1995;152:248–52.

Available online at www.sciencedirect.com
ScienceDirect
Neuroscience Research xxx (2007) xxx–xxx
Neuroscience Research
www.elsevier.com/locate/neures

Multiple-time replicability of near-infrared spectroscopy recording during prefrontal activation task in healthy men

Toshiaki Kono *, Koji Matsuo, Koichi Tsunashima, Kiyoto Kasai **, Ryu Takizawa, Mark A. Rogers, Hidenori Yamasue, Tetsu Yano, Yuji Taketani, Nobumasa Kato

Department of Neuropsychiatry, Graduate School of Medicine, The University of Tokyo, 7-3-1 Hongo, Bunkyo-ku, Tokyo 113-8655, Japan

Received 8 March 2006; accepted 12 December 2006

Abstract

Near-infrared spectroscopy (NIRS) has the potential for clinical application in neuropsychiatry because it enables non-invasive and convenient measurement of hemodynamic response to cognitive activation. Using 24-channel NIRS in 12 healthy men, we examined the replicability of oxy- and deoxy-hemoglobin concentration ([oxyHb], [deoxyHb]) changes in the prefrontal cortex during the category fluency task over four repeated sessions (each 1-week apart). Multiple methods were employed to evaluate the replicability of magnitude, location, and time course of the NIRS signals ([oxyHb], [deoxyHb]). Task performances did not differ significantly across sessions, nor were they significantly correlated with NIRS signals. Repeated measures ANOVA and variance component analysis indicated high replicability of magnitude for both NIRS measures, whereas the effect sizes of between-session differences in [oxyHb] were not negligible. The number and spatial location of significantly activated channels were sufficiently replicable for both measures, except that the across-session overlap of significantly activated channels was weak in [deoxyHb]. The time course of the activation was acceptably replicable in both measures. Taken together, these findings suggest there is considerable replicability of multiple-time measurements of prefrontal hemodynamics during cognitive activation in men. Further studies using different conditions or assessing sensitivity to longitudinal changes following interventions are necessary.

Keywords: Category fluency; Hemoglobin concentration; Practice effect; Prefrontal; Repeatability; Repeated measurement; Reproducibility; Test–retest

1. Introduction

Near-infrared spectroscopy (NIRS) is an optical technique which can non-invasively measure changes in the hemoglobin oxygenation state in human brain (Jobsis, 1977). NIRS was originally developed for clinical monitoring of tissue oxygenation (Wyatt et al., 1986); however, it has been increasingly utilized as a neuroimaging technology. NIRS takes advantage of the principle that near-infrared light is absorbed by oxygenated (oxyHb) and deoxygenated hemoglobin (deoxyHb) but not so much by other tissues. An NIRS measurement apparatus needs a pair of optodes, one emitter and one detector, placed a few centimeters apart from each other. Near-infrared light exiting the emitter optode positioned on the scalp travels through skin, skull, and brain, and is multiply scattered and partially absorbed. The residual light not absorbed by tissue exits the head and can then be detected by the detector optode (Obrig et al., 2000). Therefore, the brain region measured is supposed to be a 'banana-shaped' area between the two optodes (Gratton et al., 1994) with a depth of 0.9 cm beneath the brain surface (Villringer et al., 1997). NIRS uses two different wavelengths of near-infrared light, and can calculate changes in the concentration of oxyHb ([oxyHb]) and deoxyHb ([deoxyHb]) by means of the modified Beer–Lambert law which describes the relationship between the intensities of incident and detected light, and the fact that the absorption characteristic determined as a function of wavelength differs between oxyHb and deoxyHb.

Although the spatial resolution of NIRS is inferior to those of other functional neuroimaging methodologies such as positron-emission tomography (PET) and functional magnetic resonance imaging (fMRI), NIRS has a high time resolution of less than 0.01 s, and subjects can be scanned under natural

* Corresponding author. Tel.: +81 3 5800 9263; fax: +81 3 5800 6894.
** Co-corresponding author. Tel.: +81 3 5800 9263; fax: +81 3 5800 6894.
E-mail addresses: tkono-tky@umin.ac.jp (T. Kono), kasaik-tky@umin.ac.jp (K. Kasai).

0168-0102/$ – see front matter © 2006 Elsevier Ireland Ltd and the Japan Neuroscience Society. All rights reserved.
doi:10.1016/j.neures.2006.12.007

Please cite this article in press as: Kono, T. et al., Multiple-time replicability of near-infrared spectroscopy recording during prefrontal activation task in healthy men, Neurosci. Res. (2007), doi:10.1016/j.neures.2006.12.007

conditions (Miyai et al., 2001). Thus, NIRS is suitable for measuring change in cerebral blood volume (CBV) during cognitive tasks. With these advantages, several studies using NIRS have demonstrated an increase in [oxyHb] in the prefrontal cortex in response to cognitive activation in healthy subjects (Hoshi and Tamura, 1993; Villringer et al., 1993, 1997; Hock et al., 1995; Fallgatter and Strik, 1997, 1998; Hoshi et al., 2000) as well as differences in patterns of activation between healthy subjects and those with neuropsychiatric disorders (Okada et al., 1994, 1996; Hock et al., 1997; Fallgatter and Strik, 2000; Matsuo et al., 2000, 2002, 2004; Watanabe et al., 2003; Herrmann et al., 2004).

NIRS also has an advantage that repeated measurements in an individual are possible because it is non-invasive and NIRS devices are relatively small and portable. Hence, NIRS has the potential to be applied in clinical testing in which cognitive activations induced by the same kind of task are monitored at short-term multiple time-points (e.g., before and after a certain therapeutic intervention). However, the possibility for practice effects upon repeated testing with the same cognitive task must be considered. Previous PET and fMRI studies have demonstrated practice effects as a decrease (Jansma et al., 2001), an increase (Karni et al., 1995; Honda et al., 1998), or combination of both (Hempel et al., 2004) in cortical activation. The location of activation has also been observed to change in response to repeated testing with cognitive activation tasks (Raichle et al., 1994; Poldrack et al., 1998; Poldrack and Gabrieli, 2001).

The replicability of NIRS measures (i.e. oxyHb, deoxyHb, and totalHb (sum of oxyHb and deoxyHb)), was examined by Plichta et al. (2006). Event-related cerebral hemodynamics in the occipital cortex activated by a visual stimulation was assessed twice at an interval of 3 weeks in 12 subjects. They found good replicability at the group level in terms of single measure intraclass correlation coefficients (ICC) (0.72 and 0.52 for oxyHb and deoxyHb, respectively) when averaged across the significantly activated channels in the first session, whereas the results at the level of individual subjects were less consistent (mean Pearson correlation coefficients for oxyHb of 0.63 with 3 out of 12 subjects resulting in values around 0.4). Van de Ven et al. (2001) examined the replicability of CBV as measured by NIRS applying controlled desaturation (the O_2-method), and yielded a mean coefficient of variation (CV) of 10.0–12.6%. Another NIRS study by Claassen et al. (2006) also reported good replicability of CBV in 16 healthy elderly subjects using the O_2-method. They found CVs of 12.5% for 'repeatability' (between tests interval: 2 min), 11.7% for 'short-term reproducibility' (intervals of 20 and 40 min), and 15% for 'long-term reproducibility' (interval > 2 weeks).

To our knowledge, only one study (Watanabe et al., 2003) has preliminarily reported replicability of [oxyHb] change in the prefrontal cortex during cognitive activation tasks with a mean interval of 205 days in five healthy adults, and reported an acceptable replicability (ICC: 0.42 and 0.87 for design and letter fluency test, respectively). To date, however, no data exist concerning replicability of hemodynamic response induced by a cognitive activation task assessed systematically using NIRS. Accordingly, in the present study, we examined the replicability of hemoglobin concentration ([Hb]) change in the prefrontal cortex during a cognitive activation task over four repeated sessions (each 1-week apart) in healthy men using NIRS.

2. Materials and methods

2.1. Subjects

Twelve healthy male volunteers (age, mean [S.D.] = 28.1 [2.6] years) participated in the experiment. All were strongly right-handed as assessed with the Edinburgh Inventory (Oldfield, 1971) (laterality index > +85). They were examined by a trained psychiatrist (K.M.) using the Mini International Neuropsychiatric Interview (Sheehan et al., 1998) and were confirmed not to have any histories of neuropsychiatric disorders. All experiments in this study were conducted in accordance with the Declaration of Helsinki. Every subject was given a complete explanation of the study sufficient to their understanding, after which their written informed consent was obtained. This study was approved by the Ethical Committee of the Faculty of Medicine, The University of Tokyo (No. 670).

2.2. NIRS apparatus and measurement conditions

NIRS measurements were performed using a 24-channel instrument (ETG-100, Hitachi Medical Corporation, Tokyo, Japan). Two plastic shells each with nine individual optodes were carefully fixed with elastic straps on the left and the right forehead symmetrically. The most anterior row of optodes was

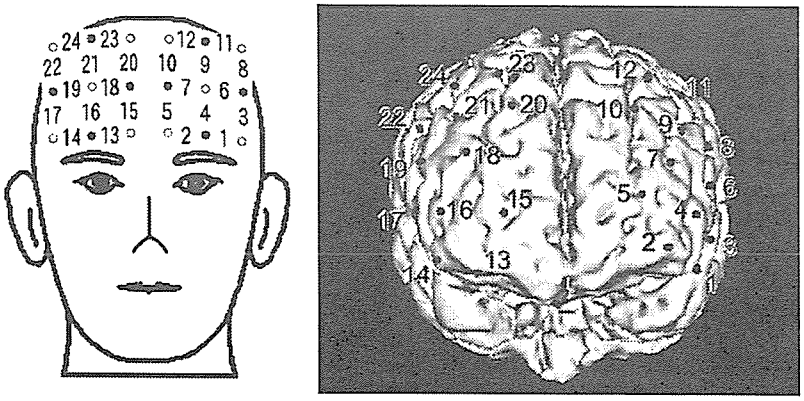

Fig. 1. Typical positions of the 24 points as indicated with digits measured by NIRS. Open and solid circles represent emitter and detector optodes, respectively (left). The positions are superimposed with red spots on a magnetic resonance image of a reconstructed cerebral cortex (right).

Please cite this article in press as: Kono, T. et al., Multiple-time replicability of near-infrared spectroscopy recording during prefrontal activation task in healthy men, Neurosci. Res. (2007), doi:10.1016/j.neures.2006.12.007

positioned along the Fp_1–Fp_2 line, according to the international 10/20 system used in electroencephalography. Typical positions of the 24 measurement points are indicated by superimposing them onto the cortical surface of a 3D-MRI image (Fig. 1). The subjects sat on a comfortable chair with their eyes open throughout the measurements.

2.3. Cognitive activation task

The category fluency task (CFT) was adopted as a cognitive activation task, and the speech–sound repetition task (SRT) was applied as a control task for the purpose of controlling for the effect of speaking. The CFT is a version of the verbal fluency task, a popular task for activating the prefrontal cortex (Audenaert et al., 2000). The subjects heard an audiotaped instruction, and were asked to repeat syllables /a/, /i/, /u/, /e/, and /o/ at approximately the same speed as an audiotaped sample in the SRT, and to generate as many words belonging to the designated category (e.g., fruits, kitchenware) as possible in the CFT. Task performance was defined as the number of correctly generated words during the CFT.

2.4. Experimental procedure

We performed four sessions of NIRS measurement at intervals of 1 week (mean [S.D.] = 7.1 [0.8] days) for each subject. A session of NIRS measurement proceeded consecutively in the following order: (1) instruction, (2) rest (2 min), (3) the SRT (1 min), (4) the CFT (1 min), and (5) the SRT (1 min). In the CFT, we designated two categories in each session. The two categories changed in turn every 30 s during the 1-min task, to reduce the time when the subjects were silent. We prepared four combinations of categories (fruits (30 s)/kitchenware (30 s); vegetables/clothes; birds/vehicles; and fishes/sports) and used each of them once

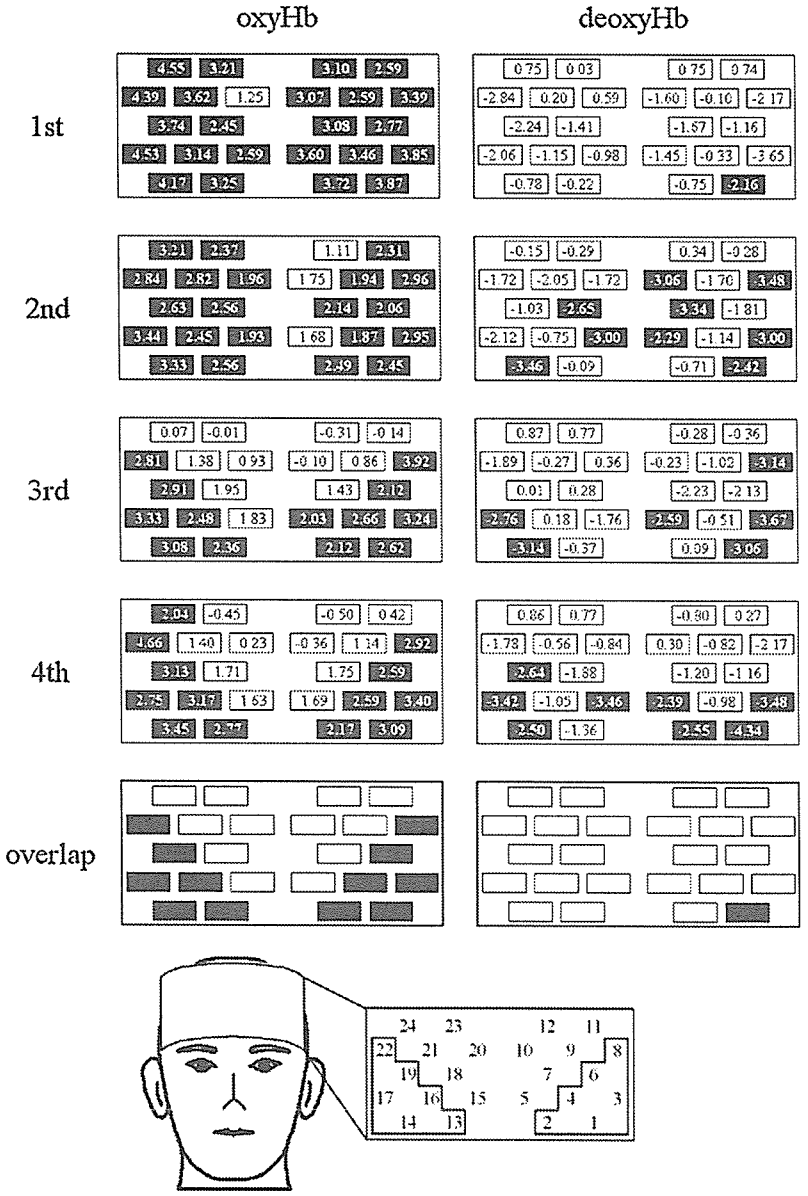

Fig. 2. Location of channels significantly activated and t-values for each NIRS measure for each recording session and those activated consistently in every session (overlap). Channels indicated as solid rectangles with t-values written in white letters in them were significantly activated, whereas those indicated as open rectangles with t-values in black letters were not. The channels are located similarly as shown in a rectangle below with the numbers of channels (the surrounded numbers correspond the channels within the region of interest).

Please cite this article in press as: Kono, T. et al., Multiple-time replicability of near-infrared spectroscopy recording during prefrontal activation task in healthy men, Neurosci. Res. (2007), doi:10.1016/j.neures.2006.12.007

with each subject, i.e. every subject experienced all eight categories in the four sessions. The order of the combinations used was randomized across the subjects.

2.5. NIRS data analyses

The NIRS data were modified to exclude short-term motion artifacts using moving average method with a window of 1 s. The obtained data were analyzed with the 'integral mode': the pre-task baseline was defined as the mean across 5 s just before the activation period (time 55–60 s of the former SRT), the post-task baseline as the mean across 5 s beginning 50 s after the activation period ended (time 50–55 s of the latter SRT), and linear fitting was performed on the data between the two baselines. Therefore, the CFT-related activation is corrected for the effect of speaking in all the NIRS data used in the analyses. Previous studies examining the relationship between NIRS signals and blood oxygenation level-dependent (BOLD) signal, measured by fMRI, during cognitive tasks have produced inconsistent results. Strangman et al. (2002) found the best correlation with oxyHb, while Huppert et al. (2006) found the best correlation with deoxyHb. Thus, we analyzed both oxyHb and deoxyHb measures throughout the analyses.

2.6. Statistical analysis

The analyses were performed with a statistical software package 'SPSS for Windows 10.1J' (SPSS Japan, Tokyo, Japan). The alpha level was set at 0.05 in the tests for statistical significance and, except for finding significantly activated channels, was not corrected for multiple comparisons because of an interest to confirm equivalence. We adopted the false discovery rate method (Singh and Dan, 2006) for multiple comparison setting q at 0.05 in finding significantly activated channels.

2.6.1. Task performance

Task performances were compared across types of category or sessions using one-way repeated measures analysis of variance (ANOVA). Then, an effect size (ES) was calculated for a difference in task performance between every two separate sessions. For ES, we regarded values of $\geq$0.65 as large, $\geq$0.35 but <0.65 as moderate, and <0.35 as small, in consideration of standard convention (Cohen, 1977).

2.6.2. Significance of NIRS signal change relative to baseline

We performed one sample t-tests (one-tailed) for [oxyHb] and [deoxyHb] changes averaged across the CFT activation period in every channel, and defined the channels in which the averaged [Hb] change was significantly positive and negative as significantly activated ones for oxyHb and deoxyHb, respectively. Then, as described in the results section, we defined a region of interest (ROI) as the channels consistently significantly activated for oxyHb in every session. The resulting ROI (left hemisphere: channels #1, 2, 3, 4, 6, 8; right hemisphere: #13, 14, 16, 17, 19, 22) (Fig. 2) was further used for analyzing the replicability of NIRS measures.

2.6.3. Correlation between task performance and NIRS signals

Pearson's correlation coefficients were calculated between task performance and averaged [oxyHb] and [deoxyHb] changes across the ROI in each single session and the four sessions combined.

2.6.4. Replicability in magnitude of activation

We evaluated the replicability of the magnitude of NIRS signal changes in three different ways.

First, we tested the differences in the averaged [oxyHb] and [deoxyHb] changes during the CFT over the four sessions using repeated measures ANOVA, for each single channel within the ROI independently and for the mean values of the six channels in each hemisphere (two within-subject factors of session and hemisphere). The absolute values of magnitudes of [Hb] change were used as both positive (for increased [Hb]) and negative (for decreased [Hb]) values.

Second, we estimated how much of the total variance of each NIRS measure could be attributed to each component of between-subject, between-session, and within-subject variance, using the data averaged for the ROI (variance component analysis).

Third, we calculated effect sizes (ESs) of all the relevant mean differences.

2.6.5. Spatial replicability

We then evaluated spatial replicability of significantly activated channels in two ways.

First, we calculated replicability indices (R_{quantity} and R_{overlap}) for each NIRS measure to quantify the replicability, extending Rombouts' ones originally defined for data in two sessions (Rombouts et al., 1997):

$$R_{\text{quantity}} = 1 - \frac{\sum_{i \neq j} |X_i - X_j|}{\sum_{i \neq j} (X_i + X_j)}$$

and

$$R_{\text{overlap}} = \frac{4X_{\text{overlap}}}{\sum_i X_i}$$

where X_i (X_j) represents the number of the activated channels in the ith (jth) session, and X_{overlap} represents that in every session consistently. Both indices can vary between 0 and 1, and high R_{quantity} and R_{overlap} indicate high replicability in terms of quantity and location, respectively, of significantly activated channels. For R_{quantity} and R_{overlap}, values of $\geq$0.8 are considered as highly replicable, $\geq$0.6 but <0.8 as moderately replicable, and <0.6 as weakly replicable. We also calculated R_{quantity} and R_{overlap} for all 24 measured channels for reference, in addition to those for the ROI.

Second, we estimated 'activation centers' in each hemisphere for each NIRS measure using the averaged [Hb] changes during the CFT in the six channels within the ROI. First of all, we assigned a frame of reference to each hemisphere such that the abscissa and the ordinate coincide with the middle horizontal and vertical rows of optodes, respectively (the origin coincides with the midmost emitter optode), assuming that the measurement areas exist on the planes composed by the axes and that the distances of any horizontally (or vertically) neighboring optodes are constant (=1). Consequently, the distance between nearest (obliquely neighboring) channels equals 1/(square root of 2) ($\approx$0.71). An activation center was defined as the mean of the coordinates of each channel weighted with the magnitude of the averaged [Hb] change in the channel. The coordinates of the activation center (x_c, y_c) were calculated as follows:

$$x_c = \frac{\sum_i x_i m_i}{\sum_i m_i}$$

$$y_c = \frac{\sum_i y_i m_i}{\sum_i m_i}$$

where m_i and (x_i, y_i) represent the magnitude of the averaged [Hb] change in and the coordinates of the ith channel, respectively. We calculated all the relevant distances of activation centers in each hemisphere for each NIRS measure.

2.6.6. Replicability in time course

We investigated temporal replicability by calculating Pearson's correlation coefficients between time series of the averaged [Hb] changes across the ROI in all the combinations of sessions for each NIRS measure.

3. Results

3.1. Task performance

Task performance of the CFT was not significantly different across types of category (mean [S.D.]; fruits and kitchenware, 20.3 [5.0]; vegetables and clothes, 22.1 [4.2]; birds and vehicles, 20.3 [5.1]; fishes and sports, 22.9 [5.8]; $F[3,33] = 2.570$, $p = 0.071$) or across sessions (1st, 21.4 [4.9]; 2nd, 21.5 [4.8]; 3rd, 22.0 [5.6]; 4th, 20.7 [5.3]; $F[3,33] = 0.374$, $p = 0.772$). The ESs were small for all the relevant mean differences (Table 1).

3.2. Significance of NIRS signal change relative to baseline

The t-tests show that, for [oxyHb], there were many channels showing significant activation associated with the cognitive

Please cite this article in press as: Kono, T. et al., Multiple-time replicability of near-infrared spectroscopy recording during prefrontal activation task in healthy men, Neurosci. Res. (2007), doi:10.1016/j.neures.2006.12.007

Table 1
Effect sizes of all the relevant mean differences in task performance and in averaged hemoglobin concentration change (mean across 12 channels within the region of interest) during the category fluency task

	1st–2nd	1st–3rd	1st–4th	2nd–3rd	2nd–4th	3rd–4th
Task performance	0.02	0.23	0.15	0.11	0.21	0.30
oxyHb	0.14	0.72	0.60	0.47	0.40	0.14
deoxyHb	0.11	0.03	0.08	0.12	0.00	0.18

task relative to baseline, while channels showing significant decreases were relatively sparse for [deoxyHb] (Fig. 2). The left hemisphere channels #1, 2, 3, 4, 6, 8, and the corresponding mirror symmetrical right hemisphere channels #13, 14, 16, 17, 19, 22 were consistently significantly activated for oxyHb in every session. Consequently, we defined these 12 channels as the ROI.

3.3. Correlation between task performance and NIRS signal

Pearson's correlation coefficients between task performance and averaged [Hb] changes were not significant for [oxyHb] ($p > 0.29$) or [deoxyHb] ($p > 0.15$).

3.4. Replicability in magnitude of activation

In the repeated measures ANOVA, the averaged [Hb] change during the CFT was not significantly different across the four

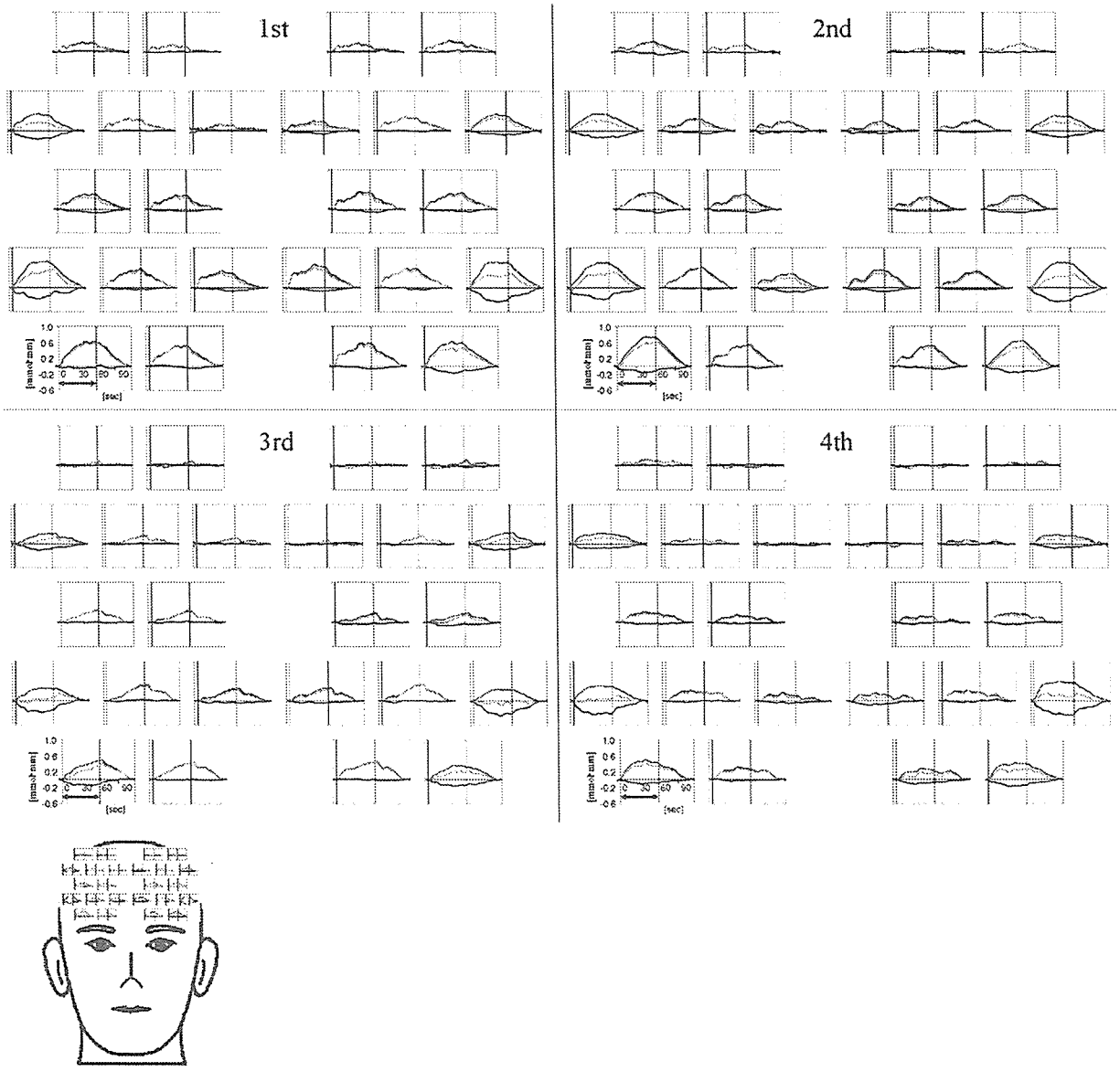

Fig. 3. Grand average waveforms of hemoglobin concentration ([Hb]) changes during the category fluency task (CFT) across all the subjects drawn for every channel in each session. [oxyHb], [deoxyHb], and [totalHb] were colored in red, blue, and green, respectively. Graphs for each channel are located similarly as shown below. The arrow drawn between the two vertical lines indicates the CFT activation period. [Hb] changes are corrected for the effect of simple speaking, using linear fitting between the pre-task baseline (the initial 5 s of the time course shown in the graphs) and the post-task baseline (the last 5 s).

Please cite this article in press as: Kono, T. et al., Multiple-time replicability of near-infrared spectroscopy recording during prefrontal activation task in healthy men, Neurosci. Res. (2007), doi:10.1016/j.neures.2006.12.007

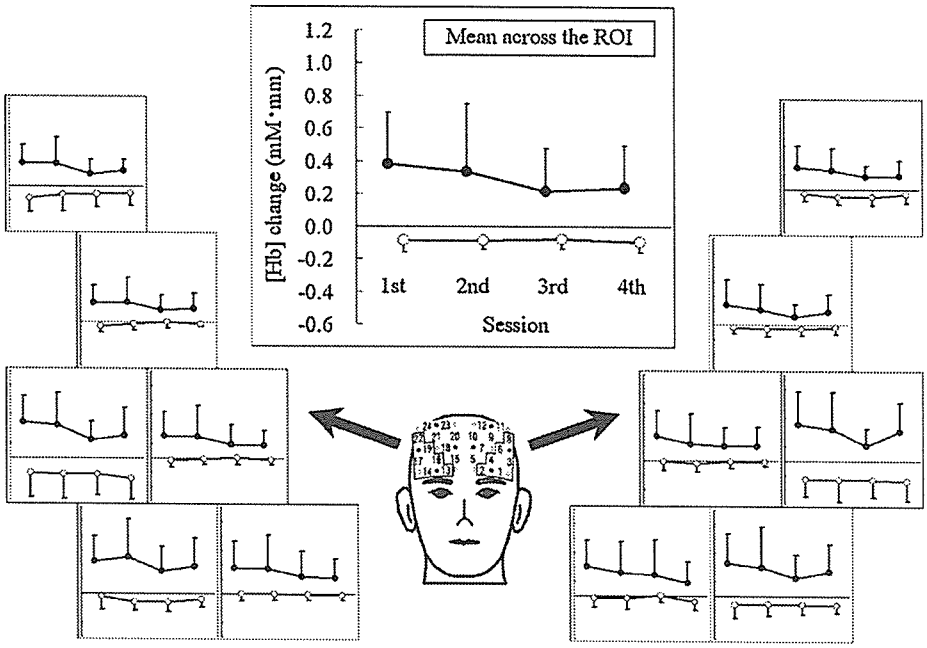

Fig. 4. Alternation in the averaged hemoglobin concentration changes during the category fluency task over the four sessions in each channel and in the mean across the region of interest. Solid and open circles represent oxygenated and deoxygenated hemoglobin, respectively. The error bars represent standard deviations.

Table 2
Number of significantly activated channels and replicability indices

NIRS measure	1st	2nd	3rd	4th	Overlap[a]	$R_{quantity}$[b]	$R_{overlap}$[b]
For the ROI							
oxyHb	12	12	12	12	12	1.00	1.00
deoxyHb	1	4	5	6	1	0.67	0.25
For all 24 channels							
oxyHb	23	20	13	13	12	0.82	0.70
deoxyHb	1	9	6	8	1	0.64	0.17

[a] The value is the number of channels activated significantly over the four sessions consistently.

[b] $R_{quantity}$ and $R_{overlap}$ are replicability indices of the quantity and the location of significantly activated channels, respectively. The formulae to calculate them are described in Section 2.6.5.

sessions in any channel within the ROI in either of oxyHb or deoxyHb (Figs. 3 and 4). In the two-way repeated measures ANOVA in consideration of laterality, there was no significant main effect of session ($F[3,33] = 2.270, 0.115$; $p = 0.099, 0.951$, for oxyHb and deoxyHb, respectively) or hemisphere ($F[1,11] = 0.374, 0.237$; $p = 0.553, 0.636$), or interaction of session and hemisphere ($F[3,33] = 0.690, 0.149$; $p = 0.565, 0.929$).

The results of variance component analysis revealed that the between-subject component contributed 66.5% of the total variance of [oxyHb] change (the proportion of between-subject component to the total variance equals single measure ICC, which means ICC = 0.665 for oxyHb), whereas the between-session component contributed only 2.9%. The within-subject component contributed the remaining 30.6%. In deoxyHb, interestingly, between-session component did not contribute to the total variance at all (0.0%), and the contribution of the between-subject component (36.7%) was conversely smaller than that of the within-subject component (63.3%).

The ESs of all the relevant mean differences in [Hb] changes were moderate to large in some combinations of sessions for [oxyHb], whereas these were consistently small for [deoxyHb] (Table 1).

3.5. Spatial replicability

$R_{quantity}$ and $R_{overlap}$ for the ROI were overall moderate to high, except for the weak $R_{overlap}$ for [deoxyHb]. Those for all the measured channels were similarly moderate to high, except for the weak $R_{overlap}$ for [deoxyHb] (Table 2).

Table 3
Mean [S.D.] values in all the relevant distance between 'activation centers' in each hemisphere

NIRS measure	Hemisphere	1st–2nd	1st–3rd	1st–4th	2nd–3rd	2nd–4th	3rd–4th
oxyHb	Left	0.26 [0.26]	0.33 [0.27]	0.39 [0.40]	0.31 [0.25]	0.24 [0.31]	0.38 [0.37]
	Right	0.20 [0.14]	0.25 [0.16]	0.29 [0.26]	0.19 [0.16]	0.30 [0.36]	0.26 [0.30]
deoxyHb	Left	0.23 [0.18]	0.33 [0.24]	0.38 [0.43]	0.31 [0.19]	0.38 [0.28]	0.27 [0.23]
	Right	0.26 [0.22]	0.38 [0.21]	0.35 [0.22]	0.36 [0.21]	0.33 [0.23]	0.30 [0.15]

Distances are expressed in relative values defined so that the distance between neighboring optodes (approximately 3 cm) equals 1.

Please cite this article in press as: Kono, T. et al., Multiple-time replicability of near-infrared spectroscopy recording during prefrontal activation task in healthy men, Neurosci. Res. (2007), doi:10.1016/j.neures.2006.12.007

Table 4
Mean [S.D.] values of all the relevant Pearson's correlation coefficients between time courses of hemoglobin concentration change

NIRS measure	1st–2nd	1st–3rd	1st–4th	2nd–3rd	2nd–4th	3rd–4th
oxyHb	0.62 [0.33]	0.65 [0.28]	0.45 [0.45]	0.43 [0.50]	0.43 [0.39]	0.35 [0.46]
deoxyHb	0.47 [0.53]	0.53 [0.37]	0.57 [0.29]	0.41 [0.39]	0.45 [0.47]	0.51 [0.36]

The mean distances of 'activated centers' ranged between 0.2 and 0.4 in both hemispheres in every combination of sessions for oxyHb and deoxyHb, without remarkable variation (Table 3).

3.6. Replicability in time course

Pearson's correlation coefficients between the time courses of [Hb] changes in every two of the four sessions were acceptable for all combinations (on average across the subjects, $r > 0.35$, d.f. = 599, $p < 0.001$) (Table 4).

4. Discussion

We evaluated the replicability of magnitude, location, and time course of NIRS signals ([oxyHb], [deoxyHb]) in the prefrontal cortex during cognitive activations over four repeated sessions employing multiple methods. In summarizing our results, repeated measures ANOVA and variance component analysis indicated high replicability of magnitude for both NIRS measures, whereas the effect sizes of between-session differences in [oxyHb] were not negligible. The number and spatial location of significantly activated channels were sufficiently replicable for both measures, except for the across-session overlap of significantly activated channels being relatively weak in [deoxyHb]. The time course of the activation was acceptably replicable in both measures. Taken together, these findings suggest considerable replicability for multiple-time measurements of prefrontal [oxyHb] and [deoxyHb] changes during cognitive activation in men.

Before discussing the replicability of NIRS signals any further, we should assess the effect of task performance. However, task performance was not significantly different across sessions. Moreover, there was no significant correlation between task performance and NIRS signals. Therefore, we can conclude that there was no meaningful effect of task performance on the NIRS data.

The repeated measures ANOVA and variance component analysis showed that the magnitudes of [oxyHb] and [deoxyHb] changes during the CFT activation were quite replicable. However, moderate to large ESs for [oxyHb] in some combinations of sessions (1st to 3rd; 1st to 4th; 2nd to 3rd; 2nd to 4th) indicated that the conclusions for the replicability of magnitude of [oxyHb] change may not be definitive.

In previous fMRI studies using cognitive activation tasks, Langenecker and Nielson (2003) demonstrated comparable magnitude of activation across two separate sessions of the Go/No-go, with an exception of stronger activation at the first test than at the retest in some frontal parts which was explained by possible extraneuronal factors such as signal-to-noise ratio or task experience. Wei et al. (2004) observed a larger contribution to variation in activation during the two-back verbal working memory task from between-subject variation than from within-subject variation (including between-session variation), although they observed a session effect as well as a subject effect in the dorsolateral prefrontal cortex that might occur as a result of difficulty in defining the region. They concluded that the findings indicate a reasonable replicability of cognitive activation over sessions.

The present study replicated the above-mentioned study by Wei et al. (2004) in terms of a large contribution of between-subject effect to the total variance in cerebral activation. However, we cannot compare the current findings directly with the previous studies because the scanning conditions are heterogeneous in multiple aspects. On that point, the study by Watanabe et al. (2003) mentioned in Section 1 to the present paper is relevant to the present study in terms of the homogenous modality (NIRS) and activation task used (fluency task), whereas the inter-session intervals were variable. As compared with the high ICC in the LFT (0.871) demonstrated in their study, the value of ICC in the CFT in the present study (0.665) is inferior. However, it may be attributed to the shorter measurement intervals in the present study, because practice effects are liable to carry over with short intervals, making cognitive activation smaller.

Concerning spatial replicability of significantly activated channels, the quantity replicability (evaluated as $R_{quantity}$) was moderate to high in both NIRS measures, whereas the location replicability (evaluated as $R_{overlap}$) was lower in deoxyHb, for not only the ROI but also all the measured channels. The spatial reliability in terms of 'activation center' was well replicated over the sessions. Our results indicate that [oxyHb] can be considered as a more replicable NIRS measure in terms of significantly activated channels than [deoxyHb]. However, a caution should be mentioned in the interpretation of the replicability of [deoxyHb], because the significantly activated channels for [deoxyHb] themselves were sparse. Thus, the activation task in our study may not be best suited for evaluating the replicability of [deoxyHb] in repeated measurements. Since Rombouts et al. (1997) introduced $R_{quantity}$ and $R_{overlap}$, similar results have been replicated in a number of fMRI and NIRS studies employing visual stimulation (e.g., Rombouts et al., 1997; Miki et al., 2000; Plichta et al., 2006). Moreover, Harrington et al. (2006) also demonstrated a higher $R_{quantity}$ as compared with $R_{overlap}$ using cognitive tasks. With regard to 'activation centers', the current result replicated a previous NIRS study by Sato et al. (2006) which demonstrated a maximum mean distance between activation centers in two sessions of 18.6 mm (=0.62) in the sensorimotor cortex during visual stimulation. On the other hand, alternation in activated regions accompanied by repeated measurements has been reported in cognitive activation task

Please cite this article in press as: Kono, T. et al., Multiple-time replicability of near-infrared spectroscopy recording during prefrontal activation task in healthy men, Neurosci. Res. (2007), doi:10.1016/j.neures.2006.12.007

paradigms (Raichle et al., 1994; Poldrack et al., 1998; Poldrack and Gabrieli, 2001). Whereas the good spatial replicability demonstrated in the present study in contrast to these previous findings may be attributed to several heterogeneous scanning conditions, it would be difficult to detect similar activation region alternation in NIRS examinations which measure not a whole brain but only surface regions of certain parts of the cerebral cortices, even if such alternation actually occurs. However, the current finding of small spatial variation within the inherent spatial resolution of NIRS in spite of repeated optode repositioning suggest sufficient spatial replicability for actual NIRS measurements in relevant cortical regions during cognitive activations.

The temporal replicability in terms of correlation coefficients between [Hb] change time courses was acceptable. However, it was inferior to that in the above-mentioned report by Sato et al. (2006) which demonstrated mean correlation coefficients around 0.85. Whereas data processing are heterogeneous between the present study and theirs on some points (they selected variable time windows from a certain extent and variable single channels allowing disagreement between sessions, both of which were of the largest absolute magnitude of [Hb] change), the current difference may be caused by the major difference in the nature of the relevant activation tasks: demand for active performance in cognitive tasks in contrast to the passiveness in sensory tasks.

There were some methodological limitations in the present study. First, the sample size was small. As far as considering the mean values of [oxyHb] change, we observed a tendency of decrease in the 3rd and 4th sessions as compared with the 1st and 2nd, though it did not reach statistical significance. It should be confirmed by examining a larger number of subjects, and using various types of cognitive activation tasks. Secondly, we examined only men, failing to examine sex differences. Women should also be included in future studies. In women, however, cognitive function may vary with menstrual cycle (Postma et al., 1999; Dietrich et al., 2001; Hausmann et al., 2002; Maki et al., 2002; Rosenberg and Park, 2002). Thus, the effects of menstrual cycle should be considered when women are included in studies.

In conclusion, the current findings suggest a considerable replicability for multiple-time measurements of prefrontal [oxyHb] and [deoxyHb] changes during cognitive activation in men. Further studies addressing various measurement conditions such as measurement interval, times of repetition and kind of activation task are necessary to identify better measurement methodologies with stable multiple-time replicability. At the same time, the sensitivity of NIRS signals to longitudinal changes in cerebral function following certain interventions (e.g., pharmacological or cognitive–behavioral interventions) should be investigated. Coupled with such evidence, our observations might provide support for clinical utility of NIRS in the field of neuropsychiatry.

Acknowledgements

This study was supported in part by Grant-in-Aid for Scientific Research on Priority Areas-Research on Pathomechanisms of Brain Disorders from the Ministry of Education, Culture, Sports, Science and Technology of Japan (No. 17025015 to K.K.), and The Japan Society for Promotion of Science (No. P05234 to M.R.). We thank Ms. Keiko Tanaka for recruiting subjects and helping to coordinate their schedules of experiment.

References

Audenaert, K., Brans, B., Van Laere, K., Lahorte, P., Versijpt, J., van Heeringen, K., Dierckx, R., 2000. Verbal fluency as a prefrontal activation probe: a validation study using ^{99}mTc-ECD brain SPET. Eur. J. Nucl. Med. 27, 1800–1808.

Claassen, J.A., Colier, W.N., Jansen, R.W., 2006. Reproducibility of cerebral blood volume measurements by near infrared spectroscopy in 16 healthy elderly subjects. Physiol. Meas. 27, 255–264.

Cohen, J., 1977. Statistical Power Analysis for the Behavioral Sciences, revised ed. Academic Press, New York, p. 40.

Dietrich, T., Krings, T., Neulen, J., Willmes, K., Erberich, S., Thron, A., Sturm, W., 2001. Effects of blood estrogen level on cortical activation patterns during cognitive activation as measured by functional MRI. NeuroImage 13, 425–432.

Fallgatter, A.J., Strik, W.K., 1997. Right frontal activation during the continuous performance test assessed with near-infrared spectroscopy in healthy subjects. Neurosci. Lett. 223, 89–92.

Fallgatter, A.J., Strik, W.K., 1998. Frontal brain activation during the Wisconsin Card Sorting Test assessed with two-channel near-infrared spectroscopy. Eur. Arch. Psychiatry Clin. Neurosci. 248, 245–249.

Fallgatter, A.J., Strik, W.K., 2000. Reduced frontal functional asymmetry in schizophrenia during a cued continuous performance test assessed with near-infrared spectroscopy. Schizophr. Bull. 26, 913–919.

Gratton, G., Maier, J.S., Fabiani, M., Mantulin, W.W., Gratton, E., 1994. Feasibility of intracranial near-infrared optical scanning. Psychopsysiology 31, 211–215.

Harrington, G.S., Buonocore, M.H., Farias, S.T., 2006. Intrasubject reproducibility of functional MR imaging activation in language tasks. Am. J. Neuroradiol. 27, 938–944.

Hausmann, M., Becker, C., Gather, U., Gunturkun, O., 2002. Functional cerebral asymmetries during the menstrual cycle: a cross-sectional and longitudinal analysis. Neuropsychologia 40, 808–816.

Hempel, A., Giesel, F.L., Garcia Caraballo, N.M., Amann, M., Meyer, H., Wustenberg, T., Essig, M., Schroder, J., 2004. Plasticity of cortical activation related to working memory during training. Am. J. Psychiatry 161, 745–747.

Herrmann, M.J., Ehlis, A.C., Fallgatter, A.J., 2004. Bilaterally reduced frontal activation during a verbal fluency task in depressed patients as measured by near-infrared spectroscopy. J. Neuropsychiatry Clin. Neurosci. 16, 170–175.

Hock, C., Muller-Spahn, F., Schuh-Hofer, S., Hofmann, M., Dirnagl, U., Villringer, A., 1995. Age dependency of changes in cerebral hemoglobin oxygenation during brain activation: a near-infrared spectroscopy study. J. Cereb. Blood Flow Metab. 15, 1103–1108.

Hock, C., Villinger, K., Muller-Spahn, F., Wenzel, R., Heekeren, H., Schuh-Hofer, S., Hofmann, M., Minoshima, S., Schwaiger, M., Dirnagl, U., Villringer, A., 1997. Decrease in parietal cerebral hemoglobin oxygenation during performance of a verbal fluency task in patients with Alzheimer's disease monitored by means of near-infrared spectroscopy (NIRS)—correlation with simultaneous rCBF-PET measurements. Brain Res. 755, 293–303.

Honda, M., Deiber, M.P., Ibanez, V., Pascual-Leone, A., Zhuang, P., Hallett, M., 1998. Dynamic cortical involvement in implicit and explicit motor sequence learning. A PET study. Brain 121, 2159–2173.

Hoshi, Y., Oda, I., Wada, Y., Ito, Y., Yamashita, Y., Oda, M., Ohta, K., Yamada, Y., Tamura, M., 2000. Visuospatial imagery is a fruitful strategy for the digit span backward task: a study with near-infrared optical tomography. Brain Res. Cogn. Brain Res. 9, 339–342.

Please cite this article in press as: Kono, T. et al., Multiple-time replicability of near-infrared spectroscopy recording during prefrontal activation task in healthy men, Neurosci. Res. (2007), doi:10.1016/j.neures.2006.12.007

Hoshi, Y., Tamura, M., 1993. Dynamic multichannel near-infrared optical imaging of human brain activity. J. Appl. Physiol. 75, 1842–1846.

Huppert, T.J., Hoge, R.D., Diamond, S.G., Franceschini, M.A., Boas, D.A., 2006. A temporal comparison of BOLD, ASL, and NIRS hemodynamic responses to motor stimuli in adult humans. NeuroImage 15, 368–382.

Jansma, J.M., Ramsey, N.F., Slagter, H.A., Kahn, R.S., 2001. Functional anatomical correlates of controlled and automatic processing. J. Cogn. Neurosci. 13, 730–743.

Jobsis, F.F., 1977. Noninvasive, infrared monitoring of cerebral and myocardial oxygen sufficiency and circulatory parameters. Science 198, 1264–1267.

Karni, A., Meyer, G., Jezzard, P., Adams, M.M., Turner, R., Ungerleider, L.G., 1995. Functional MRI evidence for adult motor cortex plasticity during motor skill learning. Nature 377, 155–158.

Langenecker, S.A., Nielson, K.A., 2003. Frontal recruitment during response inhibition in older adults replicated with fMRI. NeuroImage 20, 1384–1392.

Maki, P.M., Rich, J.B., Rosenbaum, R.S., 2002. Implicit memory varies across the menstrual cycle: estrogen effects in young women. Neuropsychologia 40, 518–529.

Matsuo, K., Kato, N., Kato, T., 2002. Decreased cerebral haemodynamic response to cognitive and physiological tasks in mood disorders as shown by near-infrared spectroscopy. Psychol. Med. 32, 1029–1037.

Matsuo, K., Kato, T., Fukuda, M., Kato, N., 2000. Alteration of hemoglobin oxygenation in the frontal region in elderly depressed patients as measured by near-infrared spectroscopy. J. Neuropsychiatry Clin. Neurosci. 12, 465–471.

Matsuo, K., Watanabe, A., Onodera, Y., Kato, N., Kato, T., 2004. Prefrontal hemodynamic response to verbal-fluency task and hyperventilation in bipolar disorder measured by multi-channel near-infrared spectroscopy. J. Affect. Disord. 82, 85–92.

Miki, A., Raz, J., van Erp, T.G., Liu, C.S., Haselgrove, J.C., Liu, G.T., 2000. Reproducibility of visual activation in functional MR imaging and effects of postprocessing. Am. J. Neuroradiol. 21, 910–915.

Miyai, I., Tanabe, H.C., Sase, I., Eda, H., Oda, I., Konishi, I., Tsunazawa, Y., Suzuki, T., Yanagida, T., Kubota, K., 2001. Cortical mapping of gait in humans: a near-infrared spectroscopic topography study. NeuroImage 14, 1186–1192.

Obrig, H., Wenzel, R., Kohl, M., Horst, S., Wobst, P., Steinbrink, J., Thomas, F., Villringer, A., 2000. Near-infrared spectroscopy: does it function in functional activation studies of the adult brain? Int. J. Psychophysiol. 35, 125–142.

Okada, F., Takahashi, N., Tokumitsu, Y., 1996. Dominance of the 'nondominant' hemisphere in depression. J. Affect. Disord. 37, 13–21.

Okada, F., Tokumitsu, Y., Hoshi, Y., Tamura, M., 1994. Impaired interhemispheric integration in brain oxygenation and hemodynamics in schizophrenia. Eur. Arch. Psychiatry Clin. Neurosci. 244, 17–25.

Oldfield, R.C., 1971. The assessment and analysis of handedness: the Edinburgh inventory. Neuropsychologia 9, 97–113.

Plichta, M.M., Herrmann, M.J., Baehne, C.G., Ehlis, A.C., Richter, M.M., Pauli, P., Fallgatter, A.J., 2006. Event-related functional near-infrared spectroscopy (fNIRS): are the measurements reliable? NeuroImage 31, 116–124.

Poldrack, R.A., Desmond, J.E., Glover, G.H., Gabrieli, J.D., 1998. The neural basis of visual skill learning: an fMRI study of mirror reading. Cereb. Cortex 8, 1–10.

Poldrack, R.A., Gabrieli, J.D., 2001. Characterizing the neural mechanisms of skill learning and repetition priming: evidence from mirror reading. Brain 124, 67–82.

Postma, A., Winkel, J., Tuiten, A., van Honk, J., 1999. Sex differences and menstrual cycle effects in human spatial memory. Psychoneuroendocrinology 24, 175–192.

Raichle, M.E., Fiez, J.A., Videen, T.O., MacLeod, A.M., Pardo, J.V., Fox, P.T., Petersen, S.E., 1994. Practice-related changes in human brain functional anatomy during nonmotor learning. Cereb. Cortex 4, 8–26.

Rombouts, S.A., Barkhof, F., Hoogenraad, F.G., Sprenger, M., Valk, J., Scheltens, P., 1997. Test–retest analysis with functional MR of the activated area in the human visual cortex. Am. J. Neuroradiol. 18, 1317–1322.

Rosenberg, L., Park, S., 2002. Verbal and spatial functions across the menstrual cycle in healthy young women. Psychoneuroendocrinology 27, 835–841.

Sato, H., Kiguchi, M., Maki, A., Fuchino, Y., Obata, A., Yoro, T., Koizumi, H., 2006. Within-subject reproducibility of near-infrared spectroscopy signals in sensorimotor activation after 6 months. J. Biomed. Opt. 11, 014021.

Sheehan, D.V., Lecrubier, Y., Sheehan, K.H., Amorim, P., Janavs, J., Weiller, E., Hergueta, T., Baker, R., Dunbar, G.C., 1998. The Mini-International Neuropsychiatric Interview (M.I.N.I.): the development and validation of a structured diagnostic psychiatric interview for DSM-IV and ICD-10. J. Clin. Psychiatry 59 (Suppl. 20), 22–33.

Singh, A.K., Dan, I., 2006. Exploring the false discovery rate in multichannel NIRS. NeuroImage 33, 542–549.

Strangman, G., Culver, J.P., Thompson, J.H., Boas, D.A., 2002. A quantitative comparison of simultaneous BOLD fMRI and NIRS recordings during functional brain activation. NeuroImage 17, 719–731.

Van de Ven, M.J., Colier, W.N., van der Sluijs, M.C., Walraven, D., Oeseburg, B., Folgering, H., 2001. Can cerebral blood volume be measured reproducibly with an improved near infrared spectroscopy system? J. Cereb. Blood Flow Metab. 21, 110–113.

Villringer, K., Minoshima, S., Hock, C., Obrig, H., Ziegler, S., Dirnagl, U., Schwaiger, M., Villringer, A., 1997. Assessment of local brain activation. A simultaneous PET and near-infrared spectroscopy study. Adv. Exp. Med. Biol. 413, 149–153.

Villringer, A., Planck, J., Hock, C., Schleinkofer, L., Dirnagl, U., 1993. Near infrared spectroscopy (NIRS): a new tool to study hemodynamic changes during activation of brain function in human adults. Neurosci. Lett. 154, 101–104.

Watanabe, A., Matsuo, K., Kato, N., Kato, T., 2003. Cerebrovascular response to cognitive tasks and hyperventilation measured by multi-channel near-infrared spectroscopy. J. Neuropsychiatry Clin. Neurosci. 15, 442–449.

Wei, X., Yoo, S.S., Dickey, C.C., Zou, K.H., Guttmann, C.R., Panych, L.P., 2004. Functional MRI of auditory verbal working memory: long-term reproducibility analysis. NeuroImage 21, 1000–1008.

Wyatt, J.S., Cope, M., Deply, D.T., Wray, S., Reynolds, E.O., 1986. Quantification of cerebral oxygenation and haemodynamics in sick newborn infants by near infrared spectrophotometry. Lancet 2, 1063–1066.

Please cite this article in press as: Kono, T. et al., Multiple-time replicability of near-infrared spectroscopy recording during prefrontal activation task in healthy men, Neurosci. Res. (2007), doi:10.1016/j.neures.2006.12.007

WILEY InterScience® DISCOVER SOMETHING GREAT

Journal of Neuroscience Research 85:479–487 (2007)

Enhanced Autophagic Cell Death in Expanded Polyhistidine Variants of HOXA1 Reduces PBX1-Coupled Transcriptional Activity and Inhibits Neuronal Differentiation

Rubigilda C. Paraguison,[1] Katsumi Higaki,[1] Kenji Yamamoto,[2] Hideo Matsumoto,[2] Tsukasa Sasaki,[3] Nobumasa Kato,[3] and Eiji Nanba[1]*

[1]Division of Functional Genomics, Research Center for Bioscience and Technology, Tottori University, Yonago, Japan
[2]Department of Psychiatry and Behavioral Sciences, Tokai University School of Medicine, Kanagawa, Japan
[3]Department of Psychiatry, Graduate School of Medicine, University of Tokyo, Tokyo, Japan

HOXA1 is a member of the homeobox gene family and is involved in early brain development. In our previous study, we identified novel variants of polyhistidine repeat tract in HOXA1 gene and showed that ectopic expression of expanded variants led to enhanced intranuclear aggregation and accelerated cell death in a time-dependent manner. Here, we further investigate the implications of polyhistidine variants on HOXA1 function. Aside from intranuclear aggregation, we observed cytosolic aggregates during the early stages of expression. Rapamycin, an autophagy inducer, resulted in decreased protein aggregation and cell death. Here, we also show an interaction between variants of HOXA1 and one of the HOX protein known cofactors, PBX1. Expanded HOXA1 variants exhibited reduced PBX1-coupled transcriptional activity through a regulatory enhancer of HOXB1. Moreover, we demonstrate that both deleted and expanded variants inhibited neurite outgrowth in retinoic acid-induced neuronal differentiation in neuroblastoma cells. These results provide further evidence that expanded polyhistidine repeats in HOXA1 enhance aggregation and cell death, resulting in impaired neuronal differentiation and cooperative binding with PBX1.

Key words: HOXA1; neuronal differentiation; PBX1; polyhistidine; protein aggregation; autophagy

HOX genes form a subset of the family of homeobox genes (Pearson et al., 2005). They are involved in specifying positional identity along the anterior-posterior axis of all bilaterian animals. In humans, the HOXA–D clusters comprise 39 HOX genes, located on chromosome regions 7p15, 17p21, 12q13, and 2q31 (Grier et al., 2005). During embryonic development, HOX genes are expressed sequentially 3′ to 5′ along the anterior to posterior axis. HOX genes contain a 61-amino-acid helix-turn-helix DNA-binding domain known as the *homeodomain* (Gehring et al., 1994). It is well established that HOX/DNA binding specificity is modified by other DNA-binding proteins, which act as cofactors. Among these are the PBX proteins, which are widely expressed in fetal and adult tissues and interact preferentially with 3′ HOX proteins (Phelan and Featherstone, 1997). PBX can modulate the affinity and stability of DNA binding and regulate transcriptional activity. The cooperative heterodimerization is carried out through a conserved protein motif found N-terminal to the Hox homeodomain (Slupsky et al., 2001; Huang et al., 2005). Interactions between PBX and HOX might also be mediated by residues of the N-terminal arm of HOX proteins (Shanmugam et al., 1997). It has been reported that PBX1 and HOXB1 can cooperatively activate the transcription through an autoregulatory element, directing spatially restricted expression of the HOXB1 gene (b1-ARE) in the developing hindbrain. However, only limited kinds of HOX can bind cooperatively with PBX (HOXA1, HOXB1, and HOXA2; Di Rocco et al.,

Contract grant sponsor: Japanese Ministry of Health, Labor and Welfare; Contract grant number: H14-kokoro-002; Contract grant sponsor: Japanese Ministry of Education, Culture Sports, Science and Technology; Contract grant number: 2005, 17659315; Contract grant number: 2004, 16012242.

*Correspondence to: Eiji Nanba, MD, PhD, Division of Functional Genomics, Research Center for Bioscience and Technology, Tottori University, 86 Nishi-machi, Yonago 683-8503, Japan.
E-mail: enanba@grape.med.tottori-u.ac.jp

Received 18 April 2006; Revised 4 October 2006; Accepted 5 October 2006

Published online 27 November 2006 in Wiley InterScience (www.interscience.wiley.com). DOI: 10.1002/jnr.21137

2001). This autoregulatory enhancer is the key regulatory element for the normal rhombomere 4 expression of Hoxb1 in the developing hindbrain, whereas Hoxa1 and Hoxb1 synergize in patterning the hindbrain cranial nerves and second pharyngeal arch (Gavalas et al., 1998).

HOXA1 is one of the first HOX genes to be expressed during embryonic development (Pearson et al., 2005). In mice, its expression starts from 7.5 dpc, and it is established in the neuroectoderm and mesoderm at 8.0 dpc. (Remacle et al., 2004). HOXA1 gene encodes two alternatively spliced mRNAs, which appear to be differentially expressed in the developing embryo. The homeodomain-containing variant 1 undergoes transcriptional activation during hindbrain development from E7 to E8.5 (Godwin et al., 1998). Functional inactivation of this gene results in prenatal lethality and numerous malformations (Lufkin et al., 1991; Carpenter et al., 1993). Hoxa1 null mice exhibit hindbrain segmentation and patterning defects that cause abnormal development of cranial nerve, cranial ganglia, and branchial arch derivatives (Chisaka et al., 1992). Furthermore, ectopic expression of Hoxa1 in transgenic mice leads to abnormalities of the developing hindbrain and ultimately results in embryonic death (Zhang et al., 1994).

HOXA1 gene contains a tract of 10-histidine repeat. In our previous study, we identified novel variants of polyhistidine tracts in HOXA1 gene in a Japanese population, and no homozygous case has been found for any of these variants (Paraguison et al., 2005). Certain individuals were heterozygous for deleted 7- and 9-histidine repeats and expanded 11- and 12-histidine repeats. Expression of expanded polyhistidine variants of HOXA1 proteins resulted in accelerated formation of ubiquitinated intranuclear aggregates and increased cell death. However, the mechanism by which this aggregation occurs is poorly understood. In this study, we showed that expression of expanded polyhistidine variants of HOXA1 in human neuroblastoma cell line SK-N-SH and embryonic carcinoma cell line P19 also caused increased intranuclear aggregation and cell death. However, there was a significant reduction of protein aggregation and cell death upon Rapamycin treatment, indicating involvement of the autophagic process. Expanded variants exhibited impaired cooperative binding with the cofactor PBX1, resulting in decreased transcriptional activity. Moreover, cells overexpressing expanded and deleted variants exhibited impaired neuronal differentiation. These data provide new insights on the function of polyhistidine variants of HOXA1 protein in neuronal cells.

MATERIALS AND METHODS

Antibodies and Reagents

The following antibodies were used: polyclonal goat anti-HOXA1 antibody (Santa Cruz Biotechnology, Santa Cruz, CA; sc-17146), monoclonal mouse anti-EGFP antibody (Santa Cruz Biotechnology, sc-9996), polyclonal rabbit anti-MAP2, H-300 (Santa Cruz Biotechnology, sc-20172), polyclonal rabbit anti PBX1, P-20 (Santa Cruz Biotechnology, sc-889), and polyclonal rabbit anti-β-tubulin H235 (Santa Cruz Biotechnology, sc-9104) and Alexa Fluor 594-conjugated anti-goat IgG, Alexa Fluor 555-conjugated anti-rabbit IgG, and Alexa Fluor 555-conjugated anti-mouse IgG (Molecular Probes, Eugene, OR). The following reagents were also used for this study: 10 μM retinoic acid (Sigma, St. Louis, MO; R2625) immediately after transfection, 10 mM 3-methyladenine (3-MA; Sigma, M9281) 15 hr prior to fixation, and 100 μM z-VAD-fmk (Promega, Madison, WI; G7231) and 2 μg/ml Rapamycin (Sigma, R0395) both right after transfection.

Expression Vectors and Reporter Construct

Human HOXA1 expression vectors were generated as described previously (Paraguison et al., 2005). The following primer sets with suitable restriction enzyme recognition sites (Sac I and Bam HI) were used to generate HOXA1 variant 1: 5′- TAGAGCTCACCATGGACAATGCAAGAATGAACTCC-3′ and 5′-ATGGATCCGTGTGGGAGGTAGTCAGAGTGTCTGA-3′. All DNA amplification steps were performed using high fidelity Pfu Ultra DNA polymerase (Stratagene, La Jolla, CA) using genomic DNA and cDNA derived from human normal lymphoblast and confirmed by sequencing (ABI 3130xl). Expression constructs were derived from CMV promoter-based expression vector, pCMV-Script (Stratagene) and pEGFP-N1 (Invitrogen, San Diego, CA). The expression plasmids pCMV-Script and pEGFP-N1 were used as empty vector controls. The luciferase reporter construct pAdMLARE containing b1-ARE and the Pbx1 expression construct pSGPbx1a were generous gifts of Prof. Zappavigna (Di Rocco et al., 2001).

Cell Culture and Transfection

COS-7 cells, murine P19 embryonal carcinoma (EC) cells, and the human neuroblastoma cell line SK-N-SH were maintained in Dulbecco's modified Eagle's medium (DMEM; Sigma; D6429) supplemented with 10% fetal bovine serum (FBS; HyClone, Logan, UT). Cultures 50–80% confluent were transfected with Fugene 6 transfection reagent (Roche, Indianapolis, IN) in accordance with the manufacturer's recommendations. For a typical experiment, 1 μg of expression vector was used in a 35-mm culture dish. For cotransfection experiments, 1 μg of reporter plasmid (pAdMLARE), 0.5 μg of HOXA1 expression construct, 1 μg of PBX1 expression construct, and 0.3 μg of pEGFP as an internal control were used in a 35-mm dish. For Western blot analyses, cells cultured in 10-cm dishes were transfected with 10 μg of plasmid construct using Fugene-6 (Roche). To initiate differentiation, SK-N-SH cells were inoculated and treated with 10 μM retinoic acid (RA), whereas P19 cells were grown in a serum-free condition. Dead cells were scored under a fluorescence microscope (Leica DMIRE2).

Luciferase Assay

After 24 hr posttransfection, the cells were harvested and lysed in Pica Gene cell culture lysis reagent (Toyo Ink, Tokyo, Japan). Luciferase assay was carried out by using a Pica Gene kit (Toyo Ink) in accordance with the manufacturer's protocol. HOXA1 cooperative expression with PBX1

using pAdMLARE reporter construct was assessed by quantitative luciferase assay with Luminescencer-PSN (Bio-Instrument ATTO AB-220). pEGFP-N1 plasmid was used as an internal control.

Immunostaining, Dead Cell Scoring, and Imaging

The cells transiently expressing HOXA1 constructs were grown in 35-mm dishes containing glass coverslips. Cells attached to the glass coverslips were washed with phosphate-buffered saline (PBS), fixed with 4% paraformaldehyde, and incubated with antibodies as described previously (Paraguison et al., 2005). Confocal scanning analysis was performed with a Leica confocal microscope (Leica TCS-SP2). The degree of protein accumulation within the cell nuclei and the cytosol of transfected cells was scored. The cells were counted from 10 randomly selected microscope fields of each sample, 15 in the case of SK-N-SH cells. The ratio of the number of cells with protein aggregation over the total number of cells was then computed. Each experiment was performed independently in triplicate.

Western Blotting and Immunoprecipitation

Posttransfected cells were harvested and lysed by sonication in a buffer containing 10 mM Tris-HCl (pH 7.4), 150 mM NaCl, 1 mM EDTA, 1 mM EGTA, and protease inhibitor cocktail (Roche). Proteins were quantified by using a protein assay rapid kit (Wako, Osaka, Japan), run on 10% or 12% SDS-PAGE gels, and transferred on PVDF membranes (Millipore, Bedford, MA; IPVH00010) by a semidry blotter (Bio-Rad, Hercules, CA). Membranes were incubated with antibodies as described previously. Protein lysates from cotransfection experiments were immunoprecipitated with anti-GFP and used for Western blotting with anti-PBX1. Polyclonal rabbit anti-MAP2 antibody was used for quantifying neuronal differentiation in SK-N-SH. Signals were detected using ECL reagent (Amersham-Pharmacia Biotech, Arlington Heights, IL) on X-ray films (Fuji). For quantification, images were analyzed in NIH Image software.

RESULTS

Expanded Polyhistidine Variants of HOXA1 Enhanced Intranuclear Protein Aggregation in Neuronal Cell Lines

We have previously reported that expanded polyhistidine variants in HOXA1 resulted in early nuclear protein aggregation and an increased cell death in COS7 cells (Paraguison et al., 2005). Increasing polyhistidine repeat length coincided with early protein aggregation and accelerated cell death. In contrast, no significant difference was observed between cells overexpressing 7-polyhistidine variant and wild-type 10-polyhistidine repeat variant.

In the current study, we observed that these nuclear aggregations were also detected in both SK-N-SH cells (Fig. 1A) and P19 cells (Fig. 1B). To rule out the possibility that these aggregates were caused by enhanced green fluorescent protein (EGFP) tagging, transfection with untagged cytomegalovirus (CMV)-driven expression of HOXA1 variants was performed in COS-7 cells. Immunostaining with anti-HOXA1/Alexa 594 anti-goat also exhibited protein aggregates 18 hr posttransfection (Fig. 1C). After 18–20 hr, cells transfected with EGFP-tagged HOXA1 proteins were analyzed for Western blotting. In lysates of cells transfected with 11- and 12-polyhistidine variants, insoluble high-molecular-weight proteins remained in the stacking gel (Fig. 1D), indicative of protein complex accumulation.

Rapamycin Cleared Protein Aggregations and Decreased Cell Death in COS-7 Cells Expressing Expanded Variants of HOXA1, Whereas 3-MA Reversed This Effect

We also attempted to determine the type of cell death occurring as a consequence of expression of HOXA1 expanded polyhistidine variants. Recently, it has been reported that autophagic cell death was partially mediated by caspase activation (Ravikumar et al., 2006). Thus, we examined whether caspase inhibition could suppress cell death by using a cell-permeable pan caspase inhibitor, z-VAD-fmk, that binds to the catalytic site of caspase proteases and can inhibit induction of apoptosis (Broustas et al., 2004). However, no significant inhibition was seen in cells treated with 100 μM z-VAD-fmk (Fig. 2A,B). Thus, we speculated that classical apoptosis is not the mechanism involved in HOXA1-related cell death.

To understand better the mechanism responsible for clearance of protein aggregates, we examined the possible role of autophagy in degrading these proteins and the effect of caspase inhibition on cell death in COS-7 cells. During our time course experiments, we observed that aggregations were present not only in the nucleus but also in the cytosol at the early stages of expression (18 hr after transfection). These cytosolic aggregates were abundant in cells expressing the expanded 12-histidine variants of HOXA1-EGFP (Fig. 2C). Aggregates gradually cleared out by the endogenous autophagic mechanism of the cell and were concentrated in the nuclei at 42 hr after transfection (Fig. 2C,D). We explored the possible involvement of the autophagic process in the clearing of protein aggregates in these cells. 3-Methyladenine (3-MA), which has an inhibitory effect on autophagy (Ravikumar et al., 2002), enhanced nuclear aggregations and cell death (Fig. 2E,F). There is a decreased rate of clearance of protein aggregates observed in 3-MA-treated cells overexpressing 12-His variant. Cytosolic aggregates around the outer perinuclear periphery are noticeable in the later stage of expression, i.e., about 42 hr, where they were supposed to be cleared out in the 3-MA nontreated transfected cells (Fig. 2F). Conversely, rapamycin, an autophagy-inducing chemical (Ravikumar et al., 2006), decreased cytosolic and nuclear aggregation that eventually reduced cell death particularly in the expanded 12-histidine variant (Fig. 2G). This suggested that clearing of HOXA1-EGFP protein aggregates was mediated by an autophagic mechanism. We

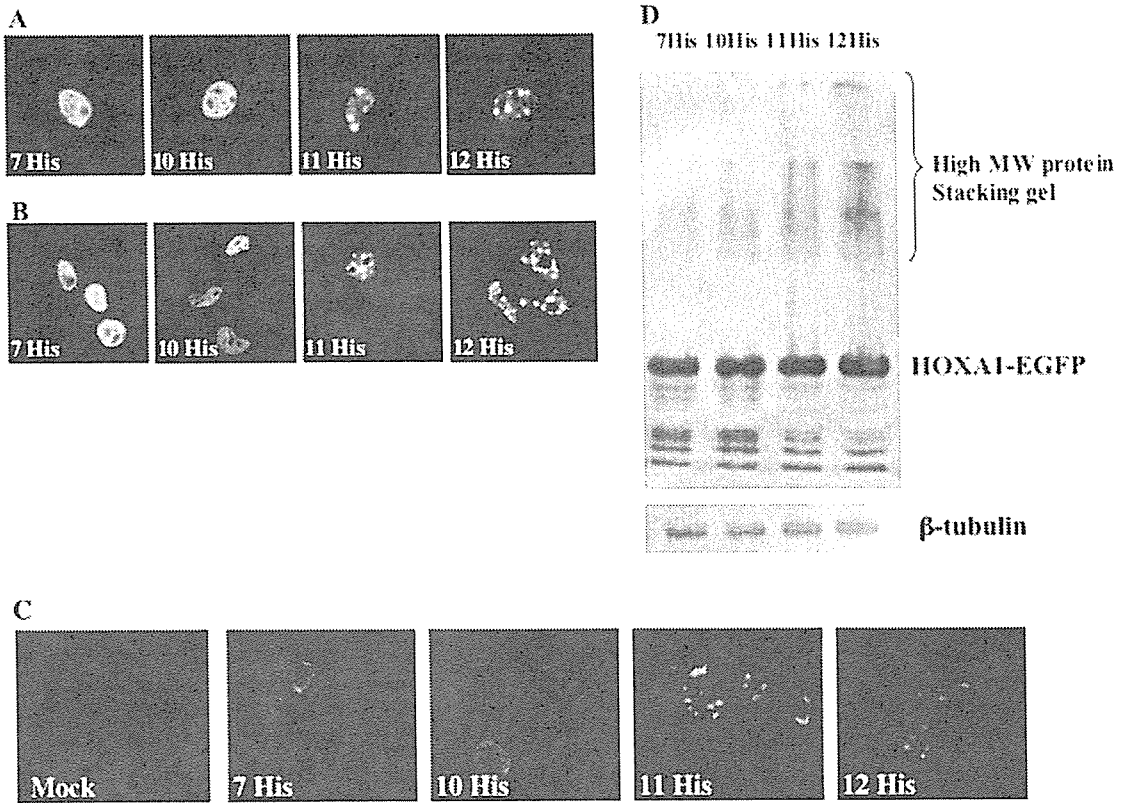

Fig. 1. Expression of HOXA1 polyhistidine expansion variants results in protein aggregation. HOXA1-EGFP construct variants were expressed in neuronal cell lines. As early as 15–20 hr after transfection, intranuclear aggregates were already detected in cells transfected with expanded HOXA1 variant. Images were taken 18 hr after transfection. EGFP fluorescent signals were visualized by confocal microscopy. **A:** Neuroblastoma cells, SK-N-SH. **B:** Embryonic carcinoma cells, P19. **C:** COS-7 cells transfected with untagged HOXA1 and immunostained with anti-HOXA1/Alexa 594 anti-goat (red signals). Fluorescence images were taken 18 hr posttransfection. **D:** 18–24-hr posttransfected cell lysates analyzed for Western blotting using anti-GFP. An increased amount of high-molecular-weight SDS-insoluble protein was detected in the stacking gel in lanes of expanded HOXA1, indicating that the length of histidine repeats is directly proportional with the degree protein accumulations. [Color figure can be viewed in the online issue, which is available at www.interscience.wiley.com.]

further noted that the autophagic clearing system was more efficient in degrading cytosolic aggregates, since autophagic vacuoles were directly accessible in the cytosol. However, the increased production of accumulated intranuclear proteins might have overloaded the autophagic clearing mechanism, thus resulting in cell death.

Fig. 2. Protein aggregations in the cytosol are cleared by an autophagic process. **A:** Right after transfection, cells were treated with 100 μM z-VAD-fmk and scored after 24 hr postransfection. z-VAD-fmk did not inhibit intranuclear protein aggregation. Mock EGFP served as a negative control. **B:** Fluorescence images of EGFP and HOXA1-EGFP 12-His variant treated with z-VAD-fmk. **C:** COS-7 cells were transfected with HOXA1-EGFP constructs at 18 hr posttransfection; cytosolic aggregates could be seen abundantly in cells transfected with HOXA1-EGFP 12-histidine variant. These aggregates were eventually cleared out after 42 hr and were mostly concentrated in the nuclei. **D:** Graph showing percentage of cells with protein aggregation and dead cells per number of EGFP-positive transfected cells at 18 and 42 hr after transfection. **E:** Transfected cells were treated with 10 mM 3-methyladenine (3-MA) 15 hr prior to fixation. HOXA1-EGFP 10-His variant-transfected cells were treated with DMSO to serve as a control for cell toxicity. 3-MA increases protein aggregations and cell death in HOXA1-EGFP-transfected COS-7 cells. Dead cells and those exhibiting nuclear and cytosolic aggregation were scored 18 hr after transfection. **F:** No protein aggregation was detected in mock-EGFP-transfected COS-7 cells treated with 3-MA; however, an increase in cell death was observed. HOXA1-EGFP 12-His variant exhibited cytosolic aggregates around the outer perinuclear periphery, which are denoted by arrows. **G:** Immediately after transfection, 10-His and 12-His repeat variants of HOXA1-EGFP-transfected COS-7 cells were treated with 2 μg/ml Rapamycin prior to fixation. Rapamycin reduces cytosolic aggregation and cell death significantly in the cells transfected with 12-His repeat variant. Dead cells and protein aggregations were scored 42 hr after transfection. Error bars represent SEM; n = 3. $*P < 0.05$, $**P < 0.01$. *P* values from a paired *t*-test in all experiments. [Color figure can be viewed in the online issue, which is available at www.interscience.wiley.com.]

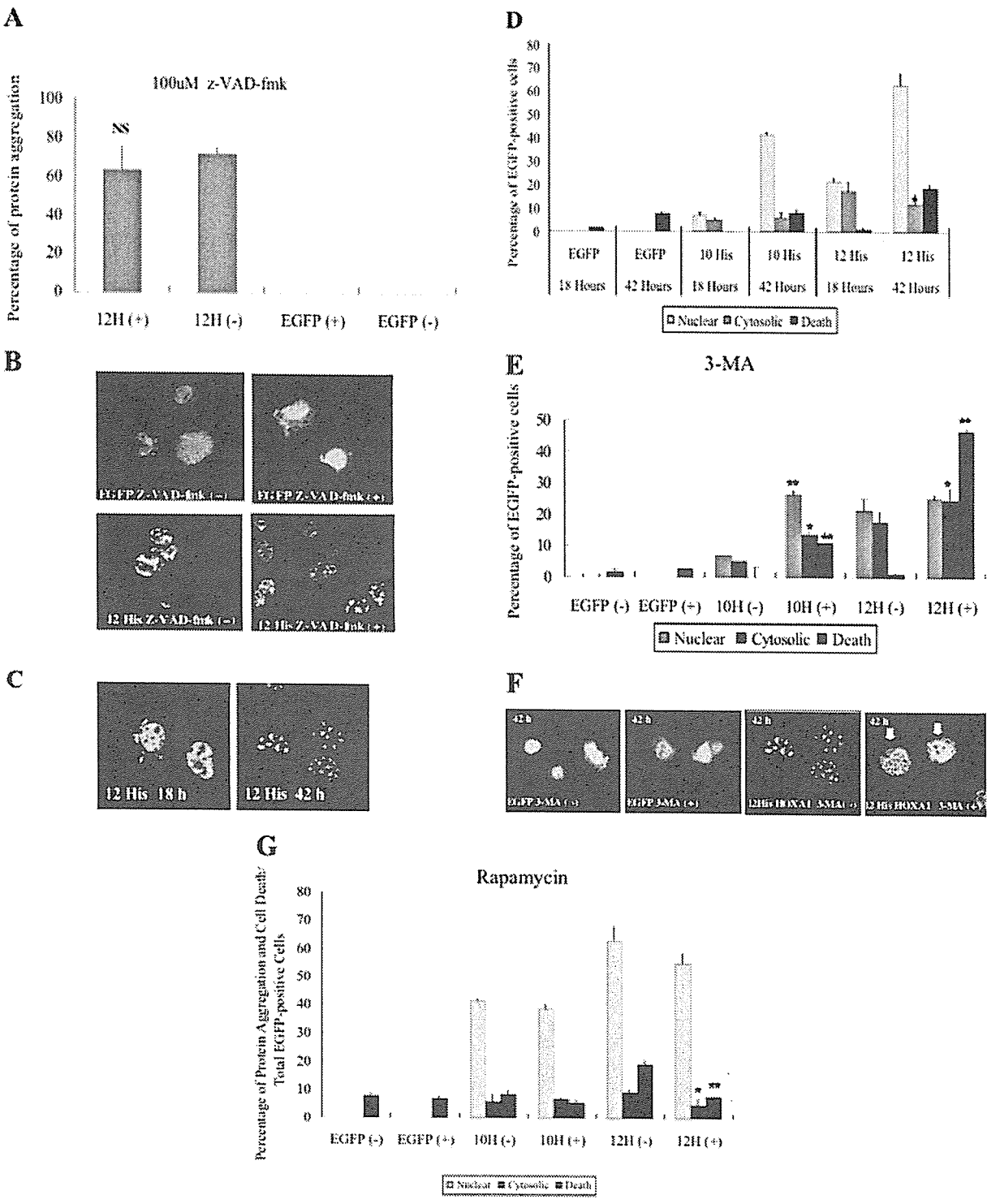
A
100uM z-VAD-fmk
Percentage of protein aggregation
NS
12H (+)
12H (-)
EGFP (+)
EGFP (-)
B
12 His Z-VAD-fmk (-)
12 His Z-VAD-fmk (+)
C
12 His 18 h
12 His 42 h
D
Percentage of EGFP-positive cells
EGFP 18 Hours
EGFP 42 Hours
10 His 18 Hours
10 His 42 Hours
12 His 18 Hours
12 His 42 Hours
Nuclear
Cytosolic
Death
E
3-MA
Percentage of EGFP-positive cells
EGFP (-)
EGFP (+)
10H (-)
10H (+)
12H (-)
12H (+)
Nuclear
Cytosolic
Death
F
G
Rapamycin
Percentage of Protein Aggregation and Cell Death/ Total EGFP-positive Cells
EGFP (-)
EGFP (+)
10H (-)
10H (+)
12H (-)
12H (+)
Nuclear
Cytosolic
Death

Figure 2.